EFFECTS OF THE PLASMA SHEATH ON ANTENNA PERFORMANCE

C. T. Swift

NASA Langley Research Center

Langley Station, Hampton, Virginia, USA

H. Hodara

National Engineering Science Company

Pasadena, California, USA

Presented at the

AGARD/IRC Meeting on "Radio Wave Propagation Factors

in Space Communications"

Rome, Italy

September 21-25, 1965

NATIONAL AERONAUTICS AND SPACE ADMINISTRATION
WASHINGTON

EFFECTS OF THE PLASMA SHEATH ON ANTENNA PERFORMANCE[1]

C. T. Swift
NASA Langley Research Center
Langley Station, Hampton, Virginia

H. Hodara
National Engineering Science Company
Pasadena, California

INTRODUCTION

Many scientific investigations have been pursued in the past few years concerning the radiation characteristics of slotted antennas immersed in a plasma. This research has, of course, been prompted by attempts to explain or predict electromagnetic effects which may occur during the reentry of space vehicles.

The analysis of the problem is conceptually simple, i.e., the wave equation is solved, and all unknown coefficients are found by applying the electro-magnetic boundary conditions at the air-plasma interface and at the aperture. However, unless idealized models of the vehicle are chosen, the evaluation of the complicated solutions of the wave equation becomes a major obstacle. In order to avoid these problems, models chosen by most investigators have been of simple geometry, namely, the coated slot on the flat ground plane and the slot on a conducting cylinder. The former is applicable to the reentry problem pro-vided the dimensions of the vehicle are much greater than a wavelength, and the latter is a reasonable choice if the wavelength is comparable to vehicle dimensions.

Radiation pattern computations constituted the earlier work in this field. The slot on the flat ground plane, coated with a gyro-plasma was analyzed by Hodara (refs. 1 and 2), and the coated cylinder was originally solved by Wait (ref. 3). Others (refs. 4, 5, 6, 7, 8, 9, and 10) have also examined these geometries from different viewpoints or to extend the results. The final expressions for the patterns reduce to relatively simple forms because of cer-tain asymptotic expansions which may be used in the far field. At least for plane geometry, patterns may be computed easily without the aid of electronic computing machines. The results are valuable because changes in the angular distribution of energy can be predicted.

However, the radiation patterns do not give a complete description of the problem. For instance, if the aperture is backed by a waveguide, the amount of power reflected back into the guide cannot be established by the patterns alone. Such information requires knowledge of the input admittance which follows from a study of the near fields.

Recently, excellent work on this subject has been done by Villeneuve (ref. 11), Galejs (refs. 12, 13, and 14) and Compton (ref. 15). All three considered a waveguide opening onto a flat ground plane; however, the differences in the formulation and results made each effort a contribution.

The only published near-field results for the cylinder is Wait's treatment of the thin half-wave axial slot radiating into free space (ref. 3, p. 48).

In this paper, the near fields of both geometries are investigated via a transfer function which algebraically relates the unknown aperture fields to those in free space. This transfer function is a matrix of computable numbers which are specified entirely by the plasma parameters, regardless of whether the plasma is homogeneous or inhomogeneous. It is important to note that the matrix is independent of the aperture excitation. Therefore, when a given plasma condition is analyzed, any aperture problem can be solved with no more degree of difficulty than the same aperture radiating into free space. The other advantage of this type of formulation is that better near-field approximations may be made without repeating the plasma solution.

To illustrate the use of these techniques, the admittance of long slots on cylinders and planes is computed. The results are compared, and the effects induced by the inhomogeneous plasma are noted. Although no computations for finite apertures are given, expressions are derived.

An appendix is also included which outlines an exact treatment of this parallel plate waveguide opening onto a flat ground plane.

RADIATION FROM SLOT ANTENNAS ON A FLAT GROUND PLANE

I. Infinite Slot with TE_x Polarization

The model shown in figure 1 consists of a conducting ground plane onto which is cut a long radiating slot excited so that $\vec{H}$ is directed along the slot. The fields are assumed to be uniformly distributed along the slot, and the exponential function $e^{j\omega t}$ is chosen to describe the time dependence. The complex permittivity of the plasma is assumed to vary only in a direction normal to the ground plane.

The scalar wave equation which describes the magnetic field in the inhomogeneous plasma is

$$\frac{\partial^2 H_x^I(y,z)}{\partial y^2} + \frac{\partial^2 H_x^I(y,z)}{\partial z^2} - \frac{1}{\epsilon}\frac{d\epsilon}{dz}\frac{\partial H_x^I(y,z)}{\partial z} + \omega^2\mu_0\epsilon(z)H_x^I(y,z) = 0 \tag{1}$$

The above equation is partially solved by expressing H_x^I as a Fourier integral, i.e.,

$$H_x^{I}(y,z) = \frac{1}{2\pi} \int_{-\infty}^{\infty} \overline{H}_x\left(k_y, z\right) e^{jk_y y} dk_y \qquad (2)$$

which leads to the total differential equation.

$$\frac{d^2 \overline{H}_x}{dz^2} - \frac{1}{\epsilon} \frac{d\epsilon}{dz} \frac{d\overline{H}_x}{dz} + \left[\omega^2 \mu_0 \epsilon(z) - k_y^2\right]\overline{H}_x = 0 \qquad (3)$$

The dielectric constant ϵ is an arbitrary function of position; therefore equation (3) must be solved by numerical means. However, since equation (3) is a second-order differential equation, an initial value of $\overline{H}_x$ and its first derivative must first be specified before any numerical work can be performed. These starting conditions are found by constructing functional solutions of E_y and H_x in regions I and II, and requiring continuity of the components at the interface $z = z_0$.

In the plasma, the fields are of the form,

$$\left.\begin{aligned} H_x^{I}(y,z) &= \frac{1}{2\pi} \int_{-\infty}^{\infty} \overline{H}_x\left(k_y, z\right) e^{jk_y y} dk_y \\[2em] E_y^{I}(y,z) &= \frac{1}{2\pi} \frac{1}{j\omega\epsilon(z)} \int_{-\infty}^{\infty} \frac{d}{dz}\overline{H}_z\left(k_y, z\right) e^{jk_y y} dk_y \end{aligned}\right\} \qquad (4)$$

And, in unbounded free space;

$$\left.\begin{aligned} H_x^{II}(y,z) &= \frac{1}{2\pi} \int_{-\infty}^{\infty} H_T\left(k_y\right) e^{jk_z z} e^{jk_y y} dk_y \\[2em] E_y^{II}(y,z) &= \frac{1}{2\pi} \frac{1}{j\omega\epsilon_0} \int_{-\infty}^{\infty} H_T\left(k_y\right) jk_z e^{jk_z z} e^{jk_y y} dk_y \end{aligned}\right\} \qquad (5)$$

where

$$k_z = \begin{cases} jk_0 \sqrt{\left(\dfrac{k_y}{k_0}\right)^2 - 1} & k_0 < |k_y| \\[2em] -k_0 \sqrt{1 - \left(\dfrac{k_y}{k_0}\right)^2} & k_0 > |k_y| \end{cases} \qquad (6)$$

The preceding choice of roots is required in order to assure outgoing, damped waves at $z = \infty$.

The boundary conditions at $z = z_0$ requires that

$$\left.\begin{array}{l} H_x{}^I\left(y,z_0\right) = H_x{}^{II}\left(y,z_0\right) \\[2mm] E_y{}^I\left(y,z_0\right) = E_y{}^{II}\left(y,z_0\right) \end{array}\right\} \tag{7}$$

Therefore, the <u>normalized</u> initial value of H_x and its derivative is:

$$\left.\begin{array}{l} g\left(k_y,z_0\right) = \dfrac{\overline{H}_x\left(k_y,z_0\right)}{H_T\left(k_y\right)e^{jk_z z_0}} = 1 \\[6mm] g'\left(k_y,z_0\right) = \dfrac{dg\left(k_y,z\right)}{dz}\bigg|_{z=z_0} = \dfrac{d}{dz}\left[\dfrac{\overline{H}_x\left(k_y,z\right)}{H_T\left(k_y\right)e^{jk_z z}}\right]_{z=z_0} = j\dfrac{\epsilon\left(z_0\right)}{\epsilon_0}\left\{\begin{array}{ll} jk_0\sqrt{\left(\dfrac{k_y}{k_0}\right)^2 - 1} & k_0 < |k_y| \\[4mm] -k_0\sqrt{1 - \left(\dfrac{k_y}{k_0}\right)^2} & k_0 > |k_0| \end{array}\right. \end{array}\right\} \tag{8}$$

If the differential equation (3) is now divided by $H_T\left(k_y\right)e^{jk_z z_0}$, normalized values of H_x can be numerically computed at $z = 0$.

The normalization constant, $H_T\left(k_y\right)e^{jk_z z_0}$ is found by completing the boundary conditions at $z = 0$.

It is of interest to note the plasma problem has been solved without any detailed thoughts given to the aperture or the method of feeding the aperture.

The transforms of the external field at the aperture are:

$$\left.\begin{array}{l} \overline{H}_x\left(k_y,0\right) = g\left(k_y,0\right)H_T\left(k_y\right)e^{jk_z z_0} \\[4mm] E_y\left(k_y,0\right) = \dfrac{-j}{k_0 Y_0 \dfrac{\epsilon(0)}{\epsilon_0}}g'\left(k_y,0\right)H_T\left(k_y\right)e^{jk_z z_0} \end{array}\right\} \tag{9}$$

In matrix form, equation (9) becomes:

$$\begin{pmatrix} \overline{H}_x\left(k_y,0\right) \\[3mm] \overline{E}_y\left(k_y,0\right) \end{pmatrix} = \begin{pmatrix} L_{11}\left(k_y\right) \\[3mm] L_{12}\left(k_y\right) \end{pmatrix} H_T e^{jk_z z_0} \tag{10}$$

4

where the matrix elements are known numbers which are defined through equations.(9). Equation (10) is nothing more than a transfer function which relates the unknown fields at the aperture to the unknown free-space Fourier coefficient $H_T(k_y)$. Therefore when the matrix elements are specified, the coated antenna is no more complicated to solve than the uncoated problem.

If the aperture is fed by a parallel plate waveguide, excited such that only TE_x modes exist in the guide, the formal solution follows by constructing interior ($z < 0$) fields and requiring continuity of $\bar{H}_x$ and $\bar{E}_y$ at $z = 0$. The interior solution will contain one unknown, namely, the reflection coefficient; therefore, the boundary conditions should, in principle, give both Γ and $H_T(k_y)$. Such a general formulation is outlined in appendix I.

The general equation developed in appendix I has not been programed; however, a first-order estimate of Γ and H_T can be achieved by intelligently guessing the electric field at the aperture. If a TEM mode is incident on the aperture, a reasonable guess for $E_y(y,0)$ is

$$E_y(y,0) = \frac{V_o}{b} \tag{11}$$

A construction of the field solutions in the guide to relate the aperture voltage V_o to the reflection coefficient is the next natural step. Use of equation (10) would then give a first-order estimate of both Γ and H_T. However, it is more conventional to solve for the external admittance of the guide. This can also be done through use of equation (10).

The Fourier transform of equation (14) is

$$\bar{E}_y\left(k_y,0\right) = V_o e^{-jk_y \frac{b}{2}} \frac{\sin\left(k_y \frac{b}{2}\right)}{k_y \frac{b}{2}} \tag{12}$$

Therefore, equation (10) may be expressed in terms of V_o as follows:

$$\begin{pmatrix} \bar{H}_x\left(k_y,0\right) \\ \bar{E}_y\left(k_y,0\right) \end{pmatrix} = \begin{pmatrix} \dfrac{L_{11}}{L_{12}} \\ 1 \end{pmatrix} V_o e^{-jk_y \frac{b}{2}} \frac{\sin\left(k_y \frac{b}{2}\right)}{k_y \frac{b}{2}} \tag{13}$$

The power per unit length radiated by the aperture is

$$P_l = \frac{1}{2} \int_{-b/2}^{b/2} H_x(y,0) E_y^*(y,0) dy = \frac{1}{2} \frac{1}{2\pi} \int_{-\infty}^{\infty} \bar{H}_x\left(k_y,0\right) \bar{E}_y^*\left(k_y,0\right) dk_y \tag{14}$$

where the dual integral representation is a statement of Parseval's theorem.

5

Using equations (13) and (14), the external aperture admittance per unit length is

$$Y_l = \frac{2P_l}{|V_o|^2} = \frac{1}{2\pi} \int_{-\infty}^{\infty} \frac{L_{11}}{L_{12}} \frac{\sin^2\left(k_y \frac{b}{2}\right)}{\left(k_y \frac{b}{2}\right)^2} dk_y$$

$$= \frac{j}{\pi} k_o Y_o \frac{\epsilon(0)}{\epsilon_o} \int_0^{\infty} \frac{g'(k_y,0)}{g(k_y,0)} \frac{\sin^2\left(k_y \frac{b}{2}\right)}{\left(k_y \frac{b}{2}\right)^2} dk_y \qquad (15)$$

In order to compute radiation patterns, $H_x^{\text{II}}(y,z)$, hence $H_T(k_y)$, must be evaluated at points far from the aperture. From equations (10) and (12),

$$H_T(k_y) = \frac{V_o e^{-j\left(k_y \frac{b}{2} + k_z z_o\right)}}{L_{12}(k_y)} \frac{\sin\left(k_y \frac{b}{2}\right)}{k_y \frac{b}{2}} \qquad (16)$$

Therefore, with the substitutions

$$\left. \begin{array}{l} z = \rho \cos \phi \\[2mm] y = \rho \sin \phi \end{array} \right\} \qquad (17)$$

the expression for $H_x^{\text{II}}(\rho,\phi)$ becomes

$$H_x^{\text{II}}(\rho,\phi) = \frac{V_o}{2\pi} \int_{-\infty}^{\infty} \left[\frac{e^{-j\left(k_y \frac{b}{2} + k_z z_o\right)}}{L_{12}(k_y)} \right] e^{j\rho\left(k_z \cos \phi + k_y \sin \phi\right)} dk_y \qquad (18)$$

where it has been assumed that

$$\frac{\sin\left(k_y \frac{b}{2}\right)}{k_y \frac{b}{2}} \cong 1 \qquad (19)$$

The integral (18) may be solved by the method of stationary phase. (See ref. 1 for application to this geometry.) The result is

6

$$H_x^{II}(\rho,\phi) \cong \frac{e^{j\frac{3\pi}{4}}}{\sqrt{\rho\lambda_o}} e^{j\left(z_o \cos\phi + \frac{b}{2}\sin\phi\right)} V_o Y_o \left\{ \frac{\epsilon(0)}{\epsilon_o} \frac{k_o \cos\phi}{g'\left(\frac{k_y}{k_o} - \sin\phi\right)} \right\} e^{-jk_o\rho} \quad (20)$$

where the magnitude of the terms in parentheses is the pattern expression, i.e.,

$$P(\phi) = k_o \left| \frac{\epsilon(0)}{\epsilon_o} \right| \frac{\cos\phi}{\left| g'\left(\frac{k_y}{k_o} - \sin\phi\right) \right|} \quad (21)$$

II. Infinite Slot With TM_x Polarization

The geometry and appropriate field representation is shown in figure 2. If the fields are polarized such that the electric field $E(y,z)$ is directed along the x-axis the wave equation for E_x^I is

$$\frac{\partial^2 E_x^I}{\partial y^2} + \frac{\partial^2 E_x^I}{\partial z^2} + \omega^2 \mu_o \epsilon E_x^I = 0 \quad (22)$$

As before, $E_x^I(y,z)$ and $E_x^{II}(y,z)$ are defined through the Fourier representation,

$$\left. \begin{aligned} E_x^I &= \frac{1}{2\pi} \int_{-\infty}^{\infty} F(k_y,z) e^{jk_y y} dk_y \\ E_x^{II} &= \frac{1}{2\pi} \int_{-\infty}^{\infty} E_T(k_y) e^{jk_z z} e^{jk_y y} dk_y \end{aligned} \right\} \quad (23)$$

Use of equations (23) then reduces equation (22) to the following equation which must be solved numerically

$$\frac{d^2 f(k_y,z)}{dz^2} + \left[\omega^2 \mu_o \epsilon(z) - k_y^2 \right] f = 0 \quad (24)$$

subject to the starting conditions,

$$f(k_y, z_0) = 1$$

$$f'(k_y, z_0) = j \begin{cases} jk_0 \sqrt{\left(\dfrac{k_y}{k_0}\right)^2 - 1} & \left|\dfrac{k_y}{k_0}\right| > 1 \\[3ex] -k_0 \sqrt{1 - \left(\dfrac{k_y}{k_0}\right)^2} & \left|\dfrac{k_y}{k_0}\right| < 1 \end{cases} \tag{25}$$

where

$$f(k_y, z) = \frac{F(k_y, z)}{E_T(k_y) e^{jk_z z_0}}$$

In matrix form, the transformed field solutions at $z = 0$ are given by

$$\begin{pmatrix} \overline{E}_x(k_y, 0) \\[2ex] \overline{H}_y(k_y, 0) \end{pmatrix} = \begin{pmatrix} f(k_y, 0) \\[2ex] -\dfrac{1}{j\omega\mu_0} f'(k_y, 0) \end{pmatrix} E_T(k_y) e^{jk_z z_0} \tag{26}$$

Now, if the electric field at the aperture corresponds to a TE_1 excitation, the following transform pairs are defined at $z = 0$

$$E_x^I(y, 0) = E_0 \cos\left(\frac{\pi y}{b}\right) \qquad -\frac{b}{2} \leqq y \leqq \frac{b}{2}$$

$$\overline{E}_x(k_y, 0) = \cdot E_0 \cdot 2\pi b \frac{\cos\left(k_y \frac{b}{2}\right)}{\pi^2 - (k_y b)^2} \tag{27}$$

and the aperture admittance per unit length is

$$Y_l = \frac{2P}{|E_0|^2} = j\frac{Y_0}{k_0} 4\pi b^2 \int_0^\infty \frac{\cos^2\left(k_y \frac{b}{2}\right)}{\left[\pi^2 - (k_y b)^2\right]^2} \frac{f'(k_y, 0)}{f(k_y, 0)} dk_y \tag{28}$$

The radiation fields, as derived from a stationary phase evaluation of E_x^{II} is given by

$$E_x^{II}(\rho, \phi) \cong E_0 e^{j\frac{\pi}{4}} \frac{e^{-jk_0\rho}}{\sqrt{\lambda_0\rho}} e^{-jk_z z_0} \frac{2\pi b \cos\left(k_0 \frac{b}{2} \sin \phi\right)}{f\left(\frac{k_y}{k_0} = -\sin \phi, 0\right)\left[\pi^2 - (k_0 b \sin \phi)^2\right]} \tag{29}$$

8

III. The General Aperture

The development of a general aperture on a ground plane, shown in figure 3, parallels the development given above, except a double Fourier integral representation is necessary because the fields depend on all three cartesian coordinates. This problem was approached by superimposing TE and TM vector potentials. By a straightforward application of the boundary conditions, it can be shown that the pertinent differential equations are

$$\left.\begin{array}{c} \dfrac{d^2 f}{dz^2} + k_o{}^2 \left[\dfrac{\epsilon(z)}{\epsilon_o} - \beta^2 \right] f = 0 \\[4mm] \dfrac{d^2 g}{dz^2} - \dfrac{1}{\epsilon(z)} \dfrac{d\epsilon(z)}{dz} \dfrac{dg}{dz} + k_o{}^2 \left[\dfrac{\epsilon(z)}{\epsilon_o} - \beta^2 \right] g = 0 \end{array}\right\} \quad (30)$$

With starting conditions

$$\left.\begin{array}{l} f\left(z_o\right) = 1 \\[2mm] f'\left(z_o\right) = j \begin{cases} jk_o\sqrt{\beta^2 - 1} & |\beta| > 1 \\[2mm] -k_o\sqrt{1 - \beta^2} & |\beta| < 1 \end{cases} \\[6mm] g\left(z_o\right) = 1 \\[2mm] g'\left(z_o\right) = j \begin{cases} jk_o n^2\left(z_o\right)\sqrt{\beta^2 - 1} & |\beta| > 1 \\[2mm] -k_o n^2\left(z_o\right)\sqrt{1 - \beta^2} & |\beta| < 1 \end{cases} \end{array}\right\} \quad (31)$$

where β is defined through the transformation $k_x = k_o\beta \cos \alpha$ and $k_y = k_o\beta \sin \alpha$.

Note that equations (30) and (31) are identical to the equations and starting conditions which were used for the infinite slot. It can therefore be concluded that when the external plasma problem is solved for the infinite slot of TE and TM polarization, it is automatically solved for the finite aperture.

The double Fourier transform of the aperture fields may also be set up in matrix form defining a transfer function which relates the aperture fields to the free-space fields. This relationship is

9

$$
\begin{pmatrix}
\bar{\bar{E}}_x(k_x,k_y,0) \\[2mm]
\bar{\bar{E}}_y(k_x,k_y,0) \\[2mm]
\bar{\bar{H}}_x(k_x,k_y,0) \\[2mm]
\bar{\bar{H}}_y(k_x,k_y,0)
\end{pmatrix}
= \frac{1}{k_0\beta^2}
\begin{pmatrix}
0 & \dfrac{-jk_x g'(0)\epsilon_0}{\epsilon(0)k_0} & 0 & -k_y f(0)\sqrt{\mu_0\epsilon_0} \\[3mm]
0 & \dfrac{-jk_y g'(0)\epsilon_0}{\epsilon(0)k_0} & 0 & k_x f(0)\sqrt{\mu_0\epsilon_0} \\[3mm]
0 & k_y g(0)\sqrt{\epsilon_0/\mu_0} & 0 & \dfrac{-jk_x f'(0)\epsilon_0}{k_0} \\[3mm]
0 & -k_x g(0)\sqrt{\epsilon_0/\mu_0} & 0 & \dfrac{-jk_y f'(0)\epsilon_0}{k_0}
\end{pmatrix}
\begin{pmatrix}
0 \\[2mm]
E_T e^{jk_z z_0} \\[2mm]
0 \\[2mm]
H_T e^{jk_z z_0}
\end{pmatrix}
\tag{32}
$$

If the aperture field corresponds to a TE_{01} excitation, then

$$
\left.
\begin{aligned}
E_x &= \frac{V}{a}\cos\frac{\pi y}{b} \\[3mm]
E_y &= 0
\end{aligned}
\right\}
\tag{33}
$$

The transforms of equations (33) are

$$
\left.
\begin{aligned}
\bar{\bar{E}}_x &= \frac{V_0}{a}\int_{-b/2}^{b/2}\int_{-a/2}^{a/2}\cos\frac{\pi y}{b}\, e^{-jk_y y} e^{-jk_x x}\, dx\, dy \\[3mm]
&= V_0\left[\frac{2\pi b\,\cos\left(k_y\dfrac{b}{2}\right)}{\pi^2-\left(k_y b\right)^2}\right]\left[\frac{\sin\left(\dfrac{k_x a}{2}\right)}{\left(\dfrac{k_x a}{2}\right)}\right] \\[3mm]
\bar{\bar{E}}_y &= 0
\end{aligned}
\right\}
\tag{34}
$$

And, the aperture admittance is

$$
Y = \frac{2P}{|V_0|^2} = \frac{1}{(2\pi)^2}\int_{-\infty}^{\infty}\int_{-\infty}^{\infty}\frac{\bar{\bar{E}}_x{}^*(k_x,k_y,0)\,\bar{\bar{H}}_y(k_x,k_y,0)}{|V_0|^2}\,dk_x\,dk_y
$$

$$
\equiv \frac{k_0^2}{(2\pi)^2}\int_0^{2\pi}\int_0^{\infty}\frac{\bar{\bar{E}}_x{}^*(\alpha,\beta,0)\,\bar{\bar{H}}_y(\alpha,\beta,0)}{|V_0|^2}\beta\, d\beta\, d\alpha
\tag{35}
$$

10

Equations (32) and (34) may be used to express E_T and H_T in terms of V_0; therefore, $H_y(k_x,k_y,0)$ may also be expressed in terms of V_0, i.e.,

$$\bar{\bar{H}}_y(k_x,k_y,0) = \frac{j\bar{\bar{E}}_x Y_0}{k_x^2 + k_y^2} \left\{ -\left(\frac{k_x}{k_0}\right)^2 \left(\frac{k_0 g}{g'}\right)\frac{\epsilon(0)}{\epsilon_0} + \left(\frac{k_y}{k_0}\right)^2 \left(\frac{f'}{k_0 f}\right) \right\} \qquad (36)$$

If equations (34) and (35) are converted to polar coordinates and substituted into equation (35), the final admittance expression is:

$$Y = jY_0(k_0 b)^2 \int_0^\infty \int_0^{2\pi} \left[\frac{\cos\left(\frac{k_0 b}{2}\sin\alpha\right)}{\pi^2 - \left(k_0 b \sin\alpha\right)^2} \right]^2 \left[\frac{\sin\left(\frac{k_0 a}{2}\cos\alpha\right)}{\left(\frac{k_0 a}{2}\cos\alpha\right)} \right]^2$$

$$\times \left\{ -\cos^2\alpha\left(\frac{k_0 g}{g'}\right)\frac{\epsilon(0)}{\epsilon_0} + \sin^2\alpha\left(\frac{f'}{k_0 f}\right) \right\} \beta \, d\beta \, d\alpha \qquad (37)$$

RADIATION FROM SLOT ANTENNAS ON A CYLINDRICAL GROUND PLANE

IV. The Infinitely Long Axial Slot on a Cylinder

The geometry is shown in figure 4. An infinitely long slot is cut into a long conducting cylinder with $\vec{H}$ directed along the axis. The structure is coated with a plasma, whose dielectric properties vary radially. It is assumed that the fields are independent of z so that H_z in regions I and II can be described by the following Fourier series in azimuth

$$\left.\begin{array}{l} H_z^I(\rho,\phi) = \displaystyle\sum_{m=-\infty}^{\infty} H_{mz}(\rho)e^{-jm\phi} \\[4mm] H_z^{II}(\rho,\phi) = \displaystyle\sum_{m=-\infty}^{\infty} C_m H_m^{(2)}\left(k_0\rho\right)e^{-jm\phi} \end{array}\right\} \qquad (38)$$

where the radial function, $H_{mz}(\rho)$ satisfied the differential equation

$$\frac{1}{\rho}\frac{d}{d\rho}\left(\rho\frac{d}{d\rho}H_{mz}\right) - \frac{1}{\epsilon}\frac{d\epsilon}{d\rho}\frac{dH_{mz}}{d\rho} + k_0^2\left[\frac{\epsilon(\rho)}{\epsilon_0} - \frac{m^2}{(k_0\rho)^2}\right]H_{mz} = 0 \qquad (39)$$

By normalizing with respect to C_m, equation (39) can be numerically integrated provided the boundary conditions are met at $\rho = b$. The continuity requirement for H_z and E_ϕ gives

$$
\left.
\begin{aligned}
h_{mz}(b) &= \frac{H_{mz}(b)}{C_m} = H_m^{(2)}(k_o b) \\[2mm]
h_{mz}'(b) &= \frac{d}{d\rho} \frac{H_m(\rho)}{C_m}\bigg|_{\rho=b} = \frac{\epsilon(b)}{\epsilon_o} H_m^{(2)}{}'(k_o b)
\end{aligned}
\right\}
\tag{40}
$$

Equations (39) and (40) then yield normalized field solutions, $h_m(a)$ and $h_m'(a)$ at the aperture.

Since the azimuthal component of the electric field in the plasma is given by

$$
E_\phi^I(\rho,\phi) = \sum_{m=-\infty}^{\infty} E_{m\phi}(\rho) e^{-jm\phi} = -\frac{1}{j\omega\epsilon(\rho)} \sum_{m=-\infty}^{\infty} \frac{dH_{mz}(\rho)}{d\rho} e^{-jm\phi}
\tag{41}
$$

the field transforms at the aperture can immediately be written as

$$
\begin{pmatrix} H_{mz}(a) \\[3mm] E_{m\phi}(a) \end{pmatrix} = \begin{pmatrix} h_{mz}(a) \\[3mm] -\dfrac{1}{j\omega\epsilon(a)} h_{mz}'(a) \end{pmatrix} C_m
\tag{42}
$$

The power per unit length radiated by the aperture is

$$
P_l = \frac{a}{2} \int_{-\phi_0/2}^{\phi_0/2} E_\phi^{I*}(a,\phi) H_z^I(a,\phi)\, d\phi
$$

$$
= \frac{a}{2} \sum_{m=-\infty}^{\infty} \sum_{m'=-\infty}^{\infty} E_{m'\phi}^{I*}(a) H_{m\phi}^I(a) \int_{-\pi}^{\pi} e^{+j(m'-m)\phi}\, d\phi
$$

$$
= \pi a \sum_{m=-\infty}^{\infty} \sum_{m'=-\infty}^{\infty} E_{m'\phi}^{I*}(a) H_{mz}^I(a) \delta_m^{m'} = \pi a \sum_{m=-\infty}^{\infty} E_{m\phi}^{I*} H_{mz}^I(a)
\tag{43}
$$

where the equivalence of the integral over physical space to the sum over mode space is nothing more than Parseval's theorem in cylindrical coordinates.

12

It is now assumed that the electric field distribution at the aperture is

$$E_\phi(a,\phi) = \frac{V_o}{a} \tag{44}$$

whose transform is

$$E_{m\phi}(a) = \frac{1}{2\pi} \int_{-\phi_o/2}^{\phi_o/2} E_\phi(a,\phi) e^{-jm\phi} d\phi$$

$$= \frac{V_o}{2\pi a} \frac{\sin\left(\frac{m\phi_o}{2}\right)}{\left(\frac{m\phi_o}{2}\right)} \tag{45}$$

From equations (42) and (45) the transform of $H_z^{\ I}$ at the aperture is

$$H_{mz}(a) = -j\omega\epsilon(a)\frac{V_o}{2\pi a} \frac{\sin\left(\frac{m\phi_o}{2}\right)}{\left(\frac{m\phi_o}{2}\right)} \frac{h_{mz}(a)}{h_{mz}{}'(a)} \tag{46}$$

Therefore, the admittance per unit length is:

$$Y_l = \frac{2P}{|V_o|^2} = -j\frac{k_o Y_o}{2\pi a} \frac{\epsilon(a)}{\epsilon_o} \sum_{m=-\infty}^{\infty} \left[\frac{\sin\left(\frac{m\phi_o}{2}\right)}{\left(\frac{m\phi_o}{2}\right)}\right]^2 \frac{h_m(a)}{h_m{}'(a)} \tag{47}$$

The radiation pattern expression is found by solving for C_m, substituting into the second of equations (38), and evaluating $H_z^{\ II}(\rho,\phi)$ in the far field (i.e., by asymptotically expanding the Hankel function). From equations (42) and (45),

$$C_m = \frac{-j\omega\epsilon(a)}{2\pi a h_m{}'(a)} V_o \frac{\sin\left(\frac{m\phi_o}{2}\right)}{\left(\frac{m\phi_o}{2}\right)} \tag{48}$$

Therefore, $H_z^{\ II}(\rho,\phi)$ in the far field is given by

$$H_z(\rho,\phi) = -j\frac{V_o Y_o}{2\pi a}\sqrt{\frac{2}{\pi k_o \rho}}\, e^{-j\left(k_o\rho - \frac{\pi}{4}\right)} \left\{ \frac{\epsilon(0)}{\epsilon_o} \sum_{m=-\infty}^{\infty} \left[\frac{\sin\left(\frac{m\phi_o}{2}\right)}{\left(\frac{m\phi_o}{2}\right)}\right] \frac{e^{-jm\left(\phi - \frac{\pi}{2}\right)}}{h_m{}'(a)} \right\} \tag{49}$$

The pattern is computed by taking the magnitude of the term in brackets.

V. The Arbitrary Aperture on a Cylindrical Ground Plane

The preferable method of approaching the problem of a general aperture radiating into a radially varying plasma as shown in figure 5 would be to construct the fields from axial TE and TM components and numerically solve the differential equations. However, such an attempt fails because the Maxwell equations will not be satisfied.

As an alternative approach (ref. 16), the inhomogeneous plasma was replaced by several homogeneous tandem layers judiciously chosen to fit the given distribution. The development of the problem follows from a straight-forward generalization of Wait (ref. 3), and will therefore only be outlined here.

Since each layer is homogeneous, the axial components of $\vec{E}$ and $\vec{H}$ completely specify the external problem, and can be written as follows:

$$\left.\begin{array}{l} E_z{}^i(\rho,\phi,z) = \dfrac{1}{j\omega\mu_0\epsilon_i} \displaystyle\sum_{m=-\infty}^{\infty} e^{-jm\phi} \int_{-\infty}^{\infty} u_i{}^2 F_m{}^i\left(k_z,\rho\right) e^{-jk_z z} dk_z \\[4mm] H_z{}^i(\rho,\phi,z) = \dfrac{1}{j\omega\mu_0\epsilon_i} \displaystyle\sum_{m=-\infty}^{\infty} e^{-jm\phi} \int_{-\infty}^{\infty} u_i{}^2 G_m{}^i\left(k_z,\rho\right) e^{-jk_z z} dk_z \end{array}\right\} \tag{50}$$

where the superscript i refers to the fields in the ith layer. When $i = 1, 2, \ldots, n$, the radial solutions of equations (50) are:

$$\left.\begin{array}{l} F_m{}^i\left(k_z,\rho\right) = a_m{}^i J_m\left(u_i\rho\right) + A_m{}^i\left(u_i\rho\right) \\[4mm] G_m{}^i\left(k_z,\rho\right) = b_m{}^i J_m\left(u_i\rho\right) + B_m{}^i\left(u_i\rho\right) \end{array}\right\} \tag{51}$$

No standing waves exist in free space ($i = n + 1$); therefore, $F_m{}^i$ and $G_m{}^i$ are of the form:

$$\left.\begin{array}{l} F_m{}^{n+1}\left(k_z,\rho\right) = c_m H_m{}^{(2)}\left(u_0\rho\right) \\[4mm] G_m{}^{m+1}\left(k_z,\rho\right) = d_m H_m{}^{(2)}\left(u_0\rho\right) \end{array}\right\} \tag{52}$$

If equations (50) are used in connection with the Maxwell equations, the azimuthal components of E and H can be computed, and the boundary conditions can therefore be stated at each interface. From the schematic shown in figure 6, the boundary conditions at $\rho = \rho_{i+i}$ are:

14

$$
\left.\begin{array}{l}
E_\phi{}^i\left(\rho_{i+1},\phi,z\right) = E_\phi{}^{i+1}\left(\rho_{i+1},\phi,z\right) \\[12pt]
E_z{}^i\left(\rho_{i+1},\phi,z\right) = E_z{}^{i+1}\left(\rho_{i+1},\phi,z\right) \\[12pt]
H_\phi{}^i\left(\rho_{i+1},\phi,z\right) = H_\phi{}^{i+1}\left(\rho_{i+1},\phi,z\right) \\[12pt]
H_z{}^i\left(\rho_{i+1},\phi,z\right) = H_z{}^{i+1}\left(\rho_{i+1},\phi,z\right)
\end{array}\right\} \tag{53}
$$

The fields are defined in terms of the unknown coefficients, a_m, b_m, A_m, and B_m; therefore, equations (53) can be expressed in terms of 4×4 matrices relating the unknowns in the ith layer to those in the $(i + 1)^{th}$ layer, i.e.,

$$
\left[A_{jk}{}^{i+1}\right]\left\{\begin{array}{c} a_m{}^i \\ A_m{}^i \\ b_m{}^i \\ B_m{}^i \end{array}\right\} = \left[B_{jk}{}^{i+1}\right]\left\{\begin{array}{c} a_m{}^{i+1} \\ A_m{}^{i+1} \\ b_m{}^{i+1} \\ B_m{}^{i+1} \end{array}\right\} \tag{54}
$$

where the A and B matrices are given explicitly in appendix III.

If another 4×4 matrix is defined such that $\left[C_{jk}{}^{i+1}\right] = \left[A_{jk}{}^{i+1}\right]^{-1}\left[B_{jk}{}^{i+1}\right]$, then it can easily be verified that

$$
\left\{\begin{array}{c} a_m{}^1 \\ A_m{}^1 \\ b_m{}^1 \\ B_m{}^1 \end{array}\right\} = \left[C_{jk}{}^2\right]\left[C_{jk}{}^3\right] \cdots \left[C_{jk}{}^{n-1}\right]\left[C_{jk}{}^n\right]\left\{\begin{array}{c} a_m{}^n \\ A_m{}^n \\ b_m{}^n \\ B_m{}^n \end{array}\right\} \tag{55}
$$

That is, the unknown coefficients in the first layer can be related directly to those in the last layer by multiplying similar 4×4 matrices.

If the boundary conditions are completed at the air-plasma interface, and if $a_m{}^1$, $A_m{}^1$, $b_m{}^1$, and $B_m{}^1$ are converted to field transforms at $\rho = a$, the following transfer function is defined

15

$$\begin{Bmatrix} \bar{\bar{E}}_{mz}(a,k_z) \\ \bar{\bar{H}}_{m\phi}(a,k_z) \\ \bar{\bar{H}}_{mz}(a,k_z) \\ \bar{\bar{E}}_{m\phi}(a,k_z) \end{Bmatrix} = \begin{bmatrix} L_{jk}(m,k_z) \end{bmatrix} \begin{Bmatrix} 0 \\ c_m(k_z) \\ 0 \\ d_m(k_z) \end{Bmatrix} \tag{56}$$

where the 4×4 L-matrix is entirely composed of specified or computable parameters (dielectric constant, Bessel functions, etc.). The L-matrix is symbolically defined in Appendix III. The admittance and patterns can be found by completing the boundary conditions at the aperture, and algebraically solving for the unknowns.

RESULTS

In order to compare the radiating characteristics of slots on flat and cylindrical ground planes under typical reentry conditions, the electron density and collision frequency profile shown in figure 7 was chosen as a coating. The slot on both ground planes was infinitely long, 0.4 inch wide (the width of a standard X-band waveguide), and polarized with the magnetic field directed along the slot. The patterns and input admittance were then computed via the methods of sections I and IV.

The radiation patterns of the coated slot on a flat ground plane are shown in figure 8. The behavior of the patterns as a function of frequency is sharply divided at the peak plasma frequency of 10.76 gc. Frequencies above this exhibit definite off-axis maxima which progress toward the axis as the frequency decreases. Whereas, below 10.76 gc, the maxima occur only at $\phi = 0$, and the radiation rapidly decays as a function of angle. The shifting of the maximum and the differences in the pattern characteristics on either side of critical frequency are exactly what one would expect if the coating were homogeneous with a plasma frequency of 10.76 gc. However, the location of the pattern maximum, which for a collisionless homogeneous plasma is given by the plane wave critical angle

$$\phi_c = \cos^{-1}(fp/f)$$

does not correlate with the results of figure 8.

The radiation patterns of the coated cylinder are shown in figure 9. Again, the radiation patterns have strikingly different characteristics, depending upon whether the propagating frequency is greater than or less than the peak plasma frequency. There is also a progression of the pattern maxima above plasma resonance, but the location cannot be predicted as easily as the plane case.

16

• . The external admittance of the cylinder is plotted as a function of frequency in figure 10. Nineteen admittance points were computed in the frequency interval of 10.0 to 11.8 gc, yet this number was insufficient to establish a smooth curve because of small-scale fluctuations; nonetheless, some interesting features are revealed. The most striking effect occurs in the region of peak critical frequency, where the conductance and susceptance suddenly decrease. Based upon some recent work by C. M. Knop, low values of admittance should be expected at critical frequency.

At frequencies above resonance, the conductance rises rapidly, but the susceptance remains relatively constant. As the frequency increases, both curves smoothly approach the no-coating values, as they should. Below resonance the curves are fluctuating too much to make any general comments.

In order to save computer time, the plane results were confined to the five points shown in figure 10. The computations are not as extensive as those for the cylinder; nevertheless, there are sufficient data to conclude that for the parameters considered here, the admittance of a slot on a plane differs from the cylinder by only a few percent over the entire frequency range.

If the losses are small (as they are for this plasma distribution), trapped waves in azimuth are supported by the cylindrical structure at frequencies above resonance. Therefore, it is conceivable that the wave interference within the cylindrical coating could be such that the difference between the admittance of this structure and that of a slot on a flat ground plane would be substantial. The results of figure 10 seem to indicate that this is not so, at least for the size cylinder considered here. It is of interest to note, however, that the greatest differences in the admittance occur at frequencies above resonance, which confirms the intuitive expectation.

The computations of the external admittance of a finite aperture, coated with the inhomogeneous plasma, have not been done; however, the ratios

$$\frac{g(\beta,0)}{g'(\beta,0)} \quad \text{and} \quad \frac{f'(\beta,0)}{f(\beta,0)}$$

appearing in the integrand of equation (37) are given as a function of β in tables I(a) through I(d). Using these tables, the double integral which defines the admittance can be numerically evaluated.

The equatorial ($\theta = \pi/2$) radiation patterns of a half-wave axial slot, coated with a homogeneous plasma, are shown in figure 11, and were derived by two independent methods. The points were derived from the bracketed term of equation (49),[2] and the solid curve was derived from the L-matrix of section V. The explicit expression for equatorial pattern, in terms of the L-matrices from the stationary phase evaluation (ref. 7) is

---

[2]In the equatorial plane, the patterns of a finite slot are identical to those of an infinitely long slot (ref. 7).

$$P\left(\frac{\pi}{2}, \phi\right) = \left(\frac{2\omega Z_0}{\pi^2}\right) \left| \sum_{m=0}^{\infty} \frac{j^m \cos m\phi}{\left(1 + \delta_0{}^m\right) L_{44}} \right|$$

The agreement is good; therefore, one method substantiates the other.

The elevation patterns shown in figure 12 were taken directly from the results of W. V. T. Rusch (ref. 6), who based his treatment on a thin sheath approximation. The use of this approximation assures that the solution within the plasma may be expanded in a Taylor series about the thickness b-a. However, as the polar angle decreases from 90° to 0°, this approximation becomes invalid. The points on figure 12 were computed from the expression[3]

$$P\left(\theta, \frac{0}{\pi}\right) = \left[\frac{2\omega Z_0 \cos\left(\frac{\pi}{2} \cos \theta\right)}{\pi^2 \sin \theta} \right] \left| \sum_{m=0}^{\infty} \frac{j^{\mp m} L_{12}}{\left(1 + \delta_0{}^m\right)\left[L_{12}L_{44} - L_{42}L_{14}\right]} \right|$$

and were normalized with respect to Rusch's on-axis value of $\omega/\omega_p = 1.048$ curve. There is reasonably good agreement at $\theta = 70°$ and $\theta = 90°$, but the results begin to deviate as θ decreases. However, this was expected, so it is reasonable to assume that the method can validly be extended to the admittance problem.

CONCLUDING REMARKS

Methods have been developed whereby the radiation patterns and near-field effects can be evaluated by solving the aperture and plasma problems independently. As a special application of these techniques, infinitely long slots on planes and cylinders, coated with a reentry plasma were analyzed, and the following conclusions were noted:

(1) If the collision frequency is low, the peak value of the plasma frequency determines the radiating characteristics of the aperture. At critical, both the patterns and admittance undergo drastic changes.

(2) A homogeneous plasma "equivalent" of the inhomogeneous plasma coating given in figure 7 will give only general trends of pattern behavior.

(3) The external admittance of the particular slotted planes and cylinders considered here differs by only a few percent.

Tables were also given, whereby the external admittance of a finite aperture on a plane coated with the plasma of figure 7 can be computed by using these tables in connection with the double integral (37).

---

[3]The positive or negative sign on j is chosen if ϕ is 0 or π, respectively.

18

The solution finite aperture on a cylinder was formulated in terms of matrix products and verified by comparing the radiation patterns with known results.

ACKNOWLEDGMENTS

APPENDIX I

LIST OF SYMBOLS

a   slot dimension along the x-axis or radius of cylinder, as appropriate

b   slot dimension along the y-axis or radial distance to air-plasma interface, as appropriate

E   electric field intensity

$\overline{E},\overline{\overline{E}}$ Fourier transforms of the electric field

E_o electric field intensity at aperture of TM_x slot

f   propagating frequency

f_p plasma frequency, $8.97 \times 10^3 \sqrt{N_e}$

H   magnetic field intensity

$\overline{H},\overline{\overline{H}}$ Fourier transforms of magnetic field

H_o field intensity of incident TEM mode in waveguide

$j = \sqrt{-1}$

k_o free-space wave number

k_x, k_y, k_z Cartesian mode numbers

m   azimuthal mode numbers

n   index of refraction or discrete mode number in waveguide, as appropriate

N_e electron density

P   power

r, θ, ϕ spherical coordinates

u   radial mode numbers

V_o applied potential on slot

x,y,z   Cartesian coordinates

Y_O •   admittance of free-space, $\sqrt{\dfrac{\epsilon_O}{\mu_O}}$

Y admittance

Z_O impedance of free-space, $\sqrt{\dfrac{\mu_O}{\epsilon_O}}$

z_O plasma thickness

$\alpha = \text{arc tan}\ \dfrac{k_y}{k_x}$

$\beta = \dfrac{1}{k_O}\ \sqrt{k_x{}^2 + k_y{}^2}$

Γ reflection coefficient

$\delta_m{}^n$ Kronecher delta $\begin{cases} 0 & (m \neq n) \\ 1 & (m = n) \end{cases}$

ϵ permittivity

ϵ_O permittivity of free space

λ_O free-space wavelength

μ_O permeability of free space

ν collision frequency

ρ, ϕ, z cylindrical coordinates

ϕ_c plane-wave critical angle

ϕ_O angular width of slot

ω angular frequency

$*$ complex conjugate

Superscripts:

I   fields within the plasma

II   fields in free space

i   fields within the ith dielectric layer

n   fields within the nth dielectric layer

Subscripts:

i   physical parameters within the ith dielectric layer

l per unit length

x,y,z vector components in the principal Cartesian directions

ρ,ϕ,z vector components in the principal cylindrical directions

  A prime denotes differentiation with respect to z or ρ, as appropriate.

22

APPENDIX II

EXACT FORMULATION OF THE INFINITE SLOT ON THE GROUND PLANE

RADIATING INTO AN INHOMOGENEOUS PLASMA

Assuming a TEM wave incident upon the aperture shown in figure 1, the pertinent internal fields at $z = 0$ are given by

$$\left. \begin{array}{l} H_x(y,0) = H_o \left[1 + \displaystyle\sum_{n=0}^{\infty} A_n \cos\left(\dfrac{n\pi y}{b}\right) \right] \\[4mm] E_y(y,0) = \dfrac{1}{j\omega\epsilon_o}\dfrac{\partial H_y}{\partial z} = -\dfrac{H_o}{Y_o}\left[1 - \displaystyle\sum_{n=0}^{\infty} A_n \dfrac{k_{nz}}{k_o} \cos\left(\dfrac{n\pi y}{b}\right) \right] \end{array} \right\} \qquad \text{(II-1)}$$

where

$$\left. \begin{array}{ll} k_{nz} = \sqrt{k_o^2 - \left(\dfrac{n\pi}{b}\right)^2} & |k_o| > \dfrac{n\pi}{b} \\[4mm] k_{nz} = j\sqrt{\left(\dfrac{n\pi}{b}\right)^2 - k_o^2} & |k_o| < \dfrac{n\pi}{b} \end{array} \right\} \qquad \text{(II-2)}$$

The external fields at the aperture are, from equation (10)

$$\left. \begin{array}{l} H_x(y,0) = \dfrac{1}{2\pi} \displaystyle\int_{-\infty}^{\infty} L_{11}(k_y) H_T e^{jk_z z_o} e^{jk_y y} dk_y \\[4mm] E_y(y,0) = \dfrac{1}{2\pi} \displaystyle\int_{-\infty}^{\infty} L_{12}(k_y) H_T e^{jk_z z_o} e^{jk_y y} dk_y \end{array} \right\} \qquad \text{(II-3)}$$

The continuity requirement on E_y gives

$$\frac{1}{2\pi} \int_{-\infty}^{\infty} L_{12}(k_y) H_T e^{jk_z z_o} e^{jk_y y} dk_y = -\frac{H_o}{Y_o} \sum_{n=0}^{\infty} \left(\delta_o^{\,n} - A_n\right)\frac{k_{nz}}{k_o} \cos\left(\frac{n\pi y}{b}\right) \qquad \text{(II-4)}$$

Multiplying equation (II-4) by $e^{-jk_y' y} dy$, and integrating with respect to y gives

$$L_{12}(k_y)H_T e^{jk_z z_0} = \frac{-H_0}{Y_0} \sum_{n=0}^{\infty} \left(\delta_0^{\ n} - A_n\right)\frac{k_{nz}}{k_0} \int_0^b \cos \frac{n\pi y}{b} e^{-jk_y y} dy \qquad (II-5)$$

where the integration of the left-hand side of the above was extended over all space because $E_y = 0$ on the ground plane.

It is now convenient to define

$$\frac{1}{b} \int_0^b \cos \frac{n\pi y}{b} e^{+jk_y y} dy = \frac{-jk_y b}{(k_y b)^2 - (n\pi)^2}\left[(-1)^n e^{jk_y b} - 1\right] = C_n(k_y) \qquad (II-6)$$

which has the property

$$\int_{-\infty}^{\infty} C_n(k_y)C_l^*(k_y) dk_y = \frac{\pi}{d}\delta_n^{\ l}\left(1 + \delta_0^{\ n}\right) \qquad (II-7)$$

that is, $C_n(k_y)$ is an orthogonal function. Therefore, in terms of $C_n(k_y)$, the continuity of E gives the following equation

$$\frac{H_T}{H_0} e^{jk_z z_0} = \frac{-b}{Y_0 L_{12}(k_y)} \sum_{n=0}^{\infty} \left(\delta_0^{\ n} - A_n\right)\frac{k_{nz}}{k_0}C_n^*(k_y) \qquad (II-8)$$

The boundary conditions for H_x is a little more difficult to apply because the magnetic field involves "mixed" boundary conditions, i.e., H_x is continuous at the aperture, and equal to the unknown surface current on the ground plane. The boundary condition must therefore be applied only over the region where the aperture exists. This is done by expanding $e^{jk_y y}$ in a cosine series over the aperture; i.e.,

$$e^{jk_y y} = \sum_{n=0}^{\infty} B_n \cos \frac{n\pi y}{b} \qquad 0 \leqq y \leqq b \qquad (II-9)$$

Use of orthogonality gives

$$B_n = \frac{2}{\left(1 + \delta_0^{\ n}\right)}C_n(k_y) \qquad (II-10)$$

Therefore,

$$e^{jk_y y} = \sum_{n=0}^{\infty} \frac{2}{\left(1 + \delta_o{}^n\right)} C_n\left(k_y\right) \cos \frac{n\pi y}{b} \qquad \text{(II-11)}$$

Use of equation (II-11) in the boundary condition for H_x, gives

$$H_o \sum_{n=0}^{\infty} \left(\delta_o{}^n + A_n\right) \cos \frac{n\pi y}{b} = \frac{1}{2\pi} \int_{-\infty}^{\infty} dk_y L_{11}\left(k_y\right) H_T e^{jk_z z_o} \sum_{n=0}^{\infty} \frac{2}{\left(1 + \delta_o{}^n\right)} C_n\left(k_y\right) \cos \frac{n\pi y}{b}$$

$$\text{(II-12)}$$

or

$$\left(\delta_o{}^n + A_n\right) = \frac{1}{\pi\left(1 + \delta_o{}^n\right)} \int_{-\infty}^{\infty} L_{11}\left(k_y\right) \frac{H_T}{H_o} e^{jk_z z_o} C_n\left(k_y\right) dk_y \qquad \text{(II-13)}$$

By substituting equation (II-8) into equation (II-13),

$$\left(\delta_o{}^n + A_n\right) = \frac{b}{Y_o \pi \left(1 + \delta_o{}^n\right)} \int_{-\infty}^{\infty} dk_y \frac{L_{11}\left(k_y\right)}{L_{12}\left(k_y\right)} C_n\left(k_y\right) \sum_{q=0}^{\infty} \left(\delta_o{}^q - A_q\right) \frac{k_{qz}}{k_o} C_q{}^*\left(k_y\right)$$

$$\text{(II-14)}$$

Now, let

$$J_{nq} = \frac{b}{Y_o \pi \left(1 + \delta_o{}^n\right)} \frac{k_{qz}}{k_o} \int_{-\infty}^{\infty} \frac{L_{11}\left(k_y\right)}{L_{12}\left(k_y\right)} C_n\left(k_y\right) C_q{}^*\left(k_y\right) dk_y \qquad \text{(II-15)}$$

The equation (II-14) becomes:

$$\left(\delta_o{}^n + A_n\right) = \sum_{q=0}^{\infty} \left(\delta_o{}^q - A_q\right) J_{nq} \qquad \text{(II-16)}$$

or,

$$\sum_{q=0}^{\infty} \left(J_{nq} + \delta_n{}^q\right) A_q = J_{no} - \delta_n{}^o \qquad \text{(II-17)}$$

Therefore, since the coefficient matrix, J_{nq} can be computed after L_{11} and L_{12} are specified, the problem reduces to solving an infinite matrix (II-16) in order to compute the unknown A_q's.

25

THE FINITE APERTURE RADIATING INTO

LAYERED DIELECTRICS

Upon applying the boundary conditions (53) at $\rho = \rho_{i+1}$, the matrix relationship between the coefficients in the ith and the $(i + 1)$st layer can be expressed in many ways; however, if closed form expressions are desired, the most profitable way seems to be

$$\left[A_{jk}{}^{i+1}\right] = \begin{bmatrix} J_m\left(u_i\rho_{i+1}\right) & H_m{}^{(2)}\left(u_i\rho_{i+1}\right) & 0 & 0 \\ u_i J_m{}'\left(u_i\rho_{i+1}\right) & u_i H_m{}^{(2)}{}'\left(u_i\rho_{i+1}\right) & 0 & 0 \\ 0 & 0 & J_m\left(u_i\rho_{i+1}\right) & H_m{}^{(2)}\left(u_i\rho_{i+1}\right) \\ 0 & 0 & u_i J_m{}'\left(u_i\rho_{i+1}\right) & u_i H_m{}^{(2)}{}'\left(u_i\rho_{i+1}\right) \end{bmatrix}$$

$$(III-1)$$

$$\left[B_{jk}{}^{i+1}\right] = \begin{bmatrix} \left(\frac{k_i u_{i+1}}{k_{i+1} u_i}\right)^2 J_m\left(u_{i+1}\rho_{i+1}\right) & \left(\frac{k_i u_{i+1}}{k_{i+1} u_i}\right)^2 H_m{}^{(2)}\left(u_{i+1}\rho_{i+1}\right) & 0 & 0 \\ u_{i+1} J_m{}'\left(u_{i+1}\rho_{i+1}\right) & u_{i+1} H_m{}^{(2)}{}'\left(u_{i+1}\rho_{i+1}\right) & \frac{j\omega\mu_o m k_z}{u_i{}^2\rho_{i+1}}\left(1 - \frac{k_i{}^2}{k_{i+1}{}^2}\right)J_m\left(u_{i+1}\rho_{i+1}\right) & \frac{j\omega\mu_o m k_z}{u_i{}^2\rho_{i+1}}\left(1 - \frac{k_i{}^2}{k_{i+1}{}^2}\right)H_m{}^{(2)}\left(u_{i+1}\rho_{i+1}\right) \\ 0 & 0 & \left(\frac{k_i u_{i+1}}{k_{i+1} u_i}\right)^2 J_m\left(u_{i+1}\rho_{i+1}\right) & \left(\frac{k_i u_{i+1}}{k_{i+1} u_i}\right)^2 H_m{}^{(2)}\left(u_{i+1}\rho_{i+1}\right) \\ -\frac{j\omega\epsilon_o m k_z k_i{}^2}{k_o{}^2 u_i{}^2\rho_{i+1}}\left(1 - \frac{k_i{}^2}{k_{i+1}{}^2}\right)J_m\left(u_{i+1}\rho_{i+1}\right) & -\frac{j\omega\epsilon_o m k_z k_i{}^2}{k_o{}^2 u_i{}^2\rho_{i+1}}\left(1 - \frac{k_i{}^2}{k_{i+1}{}^2}\right)H_m{}^{(2)}\left(u_{i+1}\rho_{i+1}\right) & u_{i+1}\left(\frac{k_i}{k_{i+1}}\right)^2 J_m{}'\left(u_{i+1}\rho_{i+1}\right) & u_{i+1}\left(\frac{k_i}{k_{i+1}}\right)^2 H_m{}^{(2)}{}'\left(u_{i+1}\rho_{i+1}\right) \end{bmatrix}$$

$$(III-2)$$

where the $\left[A_{jk}{}^{i+1}\right]$ and $\left[B_{jk}{}^{i+1}\right]$ matrices are defined in equation (54). The C matrix was defined as

$$\left[C_{jk}{}^{i+1}\right] = \left[A_{jk}{}^{i+1}\right]^{-1}\left[B_{jk}{}^{i+1}\right] \qquad (III-3)$$

---

[4]Excerpts from reference 16 were used in this appendix.

where the inverse of the A-matrix is given by

$$
\left[A_{jk}^{i+1}\right]^{-1} = \begin{bmatrix} j\frac{\pi}{2}u_1\rho_{i+1}H_m^{(2)'}(u_1\rho_{i+1}) & -j\frac{\pi}{2}\rho_{i+1}H_m^{(2)}(u_1\rho_{i+1}) & 0 & 0 \\[2ex] -j\frac{\pi}{2}u_1\rho_{i+1}J_m'(u_1\rho_{i+1}) & j\frac{\pi}{2}\rho_{i+1}J_m(u_1\rho_{i+1}) & 0 & 0 \\[2ex] 0 & 0 & j\frac{\pi}{2}u_1\rho_{i+1}H_m^{(2)'}(u_1\rho_{i+1}) & -j\frac{\pi}{2}\rho_{i+1}H_m^{(2)}(u_1\rho_{i+1}) \\[2ex] 0 & 0 & -j\frac{\pi}{2}u_1\rho_{i+1}J_m'(u_1\rho_{i+1}) & j\frac{\pi}{2}\rho_{i+1}J_m(u_1\rho_{i+1}) \end{bmatrix}
$$

$$(III-4)$$

If equation (55) is carried one step further, it follows that

$$
\begin{Bmatrix} a_m^1 \\[1ex] A_m^1 \\[1ex] b_m^1 \\[1ex] B_m^1 \end{Bmatrix} = \left[C_{jk}^2\right]\left[C_{jk}^3\right] \cdots \left[C_{jk}^{n-1}\right]\left[C_{jk}^n\right]\left[C_{jk}^{n+1}\right] \begin{Bmatrix} 0 \\[1ex] c_m \\[1ex] 0 \\[1ex] d_m \end{Bmatrix} \qquad (III-5)
$$

where use was made of the fact that

$$
\left. \begin{aligned} a_m^{n+1} &= 0 \\[1ex] A_m^{n+1} &= c_m \\[1ex] b_m^{n+1} &= 0 \\[1ex] B_m^{n+1} &= d_m \end{aligned} \right\} \qquad (III-6)
$$

describe outgoing waves in free space. From the explicit form of the field transforms, it can be shown that

$$
\begin{Bmatrix}
\overline{E}_{mz}(a,k_z) \\
\overline{H}_{m\phi}(a,k_z) \\
\overline{H}_{mz}(a,k_z) \\
\overline{E}_{m\phi}(a,k_z)
\end{Bmatrix}
=
\begin{bmatrix} D_{jk}^{\ 1} \end{bmatrix}
\begin{Bmatrix}
a_m^{\ 1} \\
A_m^{\ 1} \\
b_m^{\ 1} \\
B_m^{\ 1}
\end{Bmatrix}
\qquad (\text{III-7})
$$

where

$$
\begin{bmatrix} D_{jk}^{\ 1} \end{bmatrix}
=
\begin{bmatrix}
\left(\dfrac{u_1 k_o}{k_1}\right)^2 \dfrac{J_m(u_1 a)}{j\omega\mu_o\epsilon_o} & \left(\dfrac{u_1 k_o}{k_1}\right)^2 \dfrac{H_m^{(2)}(u_1 a)}{j\omega\mu_o\epsilon_o} & 0 & 0 \\[3mm]
-\dfrac{u_1}{\mu_o}J_m{}'(u_1 a) & -\dfrac{u_1}{\mu_o}H_m^{(2)}{}'(u_1 a) & -\dfrac{m k_z k_o^2 J_m(u_1 a)}{j\omega\mu_o\epsilon_o k_1^2 a} & -\dfrac{m k_z k_o^2}{j\omega\mu_o\epsilon_o k_1^2 a}H_m^{(2)}(u_1 a) \\[3mm]
0 & 0 & \left(\dfrac{u_1 k_o}{k_1}\right)^2 \dfrac{J_m(u_1 a)}{j\omega\mu_o\epsilon_o} & \left(\dfrac{u_1 k_o}{k_1}\right)^2 \dfrac{H_m^{(2)}(u_1 a)}{j\omega\mu_o\epsilon_o} \\[3mm]
-\dfrac{k_z m k_o^2 J_m(u_1 a)}{j\omega\mu_o\epsilon_o k_1^2} & -\dfrac{k_z m k_o^2 H_m^{(2)}(u_1 a)}{j\omega\mu_o\epsilon_o k_1^2 a} & \left(\dfrac{k_o}{k_1}\right)^2 \dfrac{u_1}{\epsilon_o}J_m{}'(u_1 a) & \left(\dfrac{k_o}{k_1}\right)^2 \dfrac{u_1}{\epsilon_o}H_m^{(2)}{}'(u_1 a)
\end{bmatrix}
$$

$$(\text{III-8})$$

Hence, the L-matrix of equation (56) is the product of the $n + 1$ matrices

$$
\begin{bmatrix} L_{jk} \end{bmatrix}
=
\begin{bmatrix} D_{jk}^{\ 1} \end{bmatrix}
\begin{bmatrix} C_{jk}^{\ 2} \end{bmatrix}
\begin{bmatrix} C_{jk}^{\ 3} \end{bmatrix}
\cdots
\begin{bmatrix} C_{jk}^{\ n} \end{bmatrix}
\begin{bmatrix} C_{jk}^{\ n+1} \end{bmatrix}
\qquad (\text{III-9})
$$

It is interesting to note that if the index of refraction of all the layers is unity, the C-matrices are unit matrices.

28

REFERENCES

1. Hodara, H.: Radiation from a Gyro-Plasma Coated Magnetic Line Source. IRE Trans. on Antennas and Propagation, vol. AP-10, No. 5, Sept. 1962, pp. 581-593.

2. Hodara, H.: Radiation from a Gyro-Plasma Sheathed Aperture. IEEE Trans. on Antennas and Propagation, vol. AP-11, no. 1, Jan. 1963, pp. 2-12.

3. Wait, James R.: Electromagnetic Radiation from Cylindrical Structures. Pergamon Press, 1959.

4. Tamir, T., and Oliner, A. A.: The Influence of Complex Waves on the Radiation Field of a Slot-Excited Plasma Layer. IRE Trans. on Antennas and Propagation, vol. AP-10, January 1962, pp. 55-65.

5. Omura, M.: Radiation Pattern of a Slit in a Ground Plane Covered by a Plasma Layer. Air Force Cambridge Res. Labs., Hanscom Field, Mass., Rept. No. AFCRL-62-958, Dec. 1962.

6. Sengupta, D. L.: The Radiation Field Produced by an Infinite Slot in an Infinite Cylinder Surrounded by a Homogeneous Plasma Sheath, Radar Lab., Univ. of Mich., Ann Arbor, Rept. No. 4563-35-T, May 1963.

7. Knop, Charles M.: The Radiation Fields from a Circumferential Slot on a Metal Cylinder Coated with a Lossy Dielectric. IRE Trans. on Antennas and Propagation., vol. AP-9, no. 6, November 1961, pp. 535-545.

8. Rusch, W. V. T.: Radiation from a Plasma-Clad Axially Slotted Cylinder. USCEC Rep. 82-201 (AFCRL 714), Univ. of Southern California, May 1962.

9. Harris, J. H.: Radiation Through Cylindrical Plasma Sheaths. Sci. Rep. No. 2, (AFCRL-62-976), Hughes Aircraft Co., August 1962.

10. Swift, Calvin T.: Radiation From Slotted-Cylinder Antennas in a Re-entry Plasma Environment. NASA TN D-2187, February 1964.

11. Villeneuve, A. T.: Admittance of Waveguide Radiating into Plasma Environment. Sci. Rep. No. 6 (ARCRL-63-540), Hughes Aircraft Co., October 1963.

12. Galejs, J.: Admittance of Annular Slot Antennas Radiating into a Plasma Layer. Project No. 125, Applied Research Laboratory, Sylvania Electronic Systems, July 30, 1963.

13. Galejs, J.: Admittance of a Waveguide Radiation into Stratified Plasma. Project No. 125, Applied Research Laboratory, Sylvania Electronic Systems, June 1963.

14. Galejs, J.: Slot Antenna Impedance for Plasma Layers. Applied Research Laboratory, Sylvania Electronic Systems, July 23, 1963.

15. Compton, R. T.: The Admittance of Aperture Antennas Radiating Into Lossy Media., Ohio State Univ., Rep. 1691-5, March 15, 1964.

16. Swift, Calvin T.: Radiation From Slotted-Cylinder Antennas, Coated with Concentric Layers of Dielectric Material. Master of Science Thesis, V.P.I., April 1965.

TABLE I.- TABLES OF $\dfrac{g(\beta,0)}{g'(\beta,0)}$ AND $\dfrac{f'(\beta,0)}{f(\beta,0)}$ FOR THE INHOMOGENEOUS

PLASMA GIVEN IN FIGURE 7

(a) f = 10.00 gc

β	$\dfrac{g(\beta,0)}{g'(\beta,0)}$	$\dfrac{f'(\beta,0)}{f(\beta,0)}$
0	0.035 + j0.163	-0.424 - j0.844
0.050	0.034 + j0.164	-0.427 - j0.842
0.100	0.030 + j0.166	-0.433 - j0.836
0.150	0.023 + j0.168	-0.444 - j0.825
0.200	0.014 + j0.171	-0.460 - j0.811
0.225	0.009 + j.0172	-0.469 - j0.803
0.250	0.003 + j0.174	-0.480 - j0.793
0.275	-0.004 + j0.175	-0.492 - j0.783
0.300	-0.011 + j0.176	-0.504 - j0.771
0.325	-0.018 + j0.176	-0.518 - j0.759
0.350	-0.026 + j0.176	-0.534 - j0.746
0.375	-0.034 + j0.176	-0.550 - j0.732
0.400	-0.042 + j0.175	-0.568 - j0.716
0.425	-0.050 + j0.173	-0.586 - j0.700
0.450	-0.058 + j0.171	-0.606 - j0.684
0.475	-0.067 + j0.169	-0.627 - j0.666
0.500	-0.074 + j0.166	-0.650 - j0.647
0.550	-0.089 + j0.159	-0.698 - j0.608
0.600	-0.103 + j0.150	-0.752 - j0.565
0.650	-0.114 + j0.141	-0.810 - j0.520
0.700	-0.124 + j0.131	-0.874 - j0.471
0.800	-0.138 + j0.111	-1.016 - j0.364
0.900	-0.147 + j0.093	-1.180 - j0.240
1.000	-0.152 + j0.082	-1.364 - j0.002
1.200	-0.156 + j0.048	-2.027 - j0.001
1.400	-0.150 + j0.031	-2.508 - j0.001
1.600	-0.144 + j0.021	-2.966 - j0.001
1.800	-0.138 + j0.014	-3.413 - j0.001
2.000	-0.133 + j0.010	-3.855 - j0.001
2.500	-0.121 + j0.005	-4.946 - j0.000
3.000	-0.110 + j0.002	-6.028 - j0.000
3.500	-0.101 + j0.001	-7.102 - j0.000
4.000	-0.092 + j0.001	-8.171 - j0.000

TABLE I.- TABLES OF $\dfrac{g(\beta,0)}{g'(\beta,0)}$ AND $\dfrac{f'(\beta,0)}{f(\beta,0)}$ FOR THE INHOMOGENEOUS

PLASMA GIVEN IN FIGURE 7 - Continued

(b)   f = 10.73 gc

β	$\dfrac{g(\beta,0)}{g'(\beta,0)}$	$\dfrac{f'(\beta,0)}{f(\beta,0)}$
0	0.049 + j0.191	-0.293 - j0.970
0.050	0.043 + j0.195	-0.295 - j0.967
0.100	0.026 + j0.205	-0.302 - j0.960
0.150	-0.002 + j0.215	-0.315 - j0.948
0.200	-0.041 + j0.221	-0.332 - j0.931
0.225	-0.062 + j0.220	-0.343 - j0.921
0.250	-0.083 + j0.216	-0.355 - j0.909
0.275	-0.103 + j0.210	-0.368 - j0.897
0.300	-0.122 + j0.201	-0.382 - j0.883
0.325	-0.138 + j0.190	-0.398 - j0.868
0.350	-0.152 + j0.179	-0.415 - j0.852
0.375	-0.164 + j0.166	-0.434 - j0.835
0.400	-0.174 + j0.154	-0.453 - j0.817
0.425	-0.181 + j0.142	-0.474 - j0.798
0.450	-0.187 + j0.131	-0.497 - j0.778
0.475	-0.192 + j0.120	-0.521 - j0.757
0.500	-0.195 + j0.110	-0.546 - j0.735
0.550	-0.199 + j0.092	-0.601 - j0.688
0.600	-0.200 + j0.078	-0.662 - j0.637
0.650	-0.200 + j0.066	-0.728 - j0.584
0.700	-0.199 + j0.056	-0.801 - j0.527
0.800	-0.196 + j0.041	-0.964 - j0.403
0.900	-0.191 + j0.031	-1.152 - j0.262
1.000	-0.187 + j0.024	-1.364 - j0.002
1.200	-0.178 + j0.014	-2.095 - j0.001
1.400	-0.169 + j0.008	-2.626 - j0.001
1.600	-0.161 + j0.005	-3.128 - j0.001
1.800	-0.153 + j0.003	-3.616 - j0.001
2.000	-0.145 + j0.002	-4.097 - j0.000
2.500	-0.128 + j0.000	-5.281 - j0.000
3.000	-0.114 + j0.000	-6.448 - j0.000
3.500	-0.102 + j0.000	-7.606 - j0.000
4.000	-0.092 + j0.000	-8.756 - j0.000

32

TABLE I.- TABLES OF $\dfrac{g(\beta,0)}{g'(\beta,0)}$ AND $\dfrac{f'(\beta,0)}{f(\beta,0)}$ FOR THE INHOMOGENEOUS

PLASMA GIVEN IN FIGURE 7 - Continued
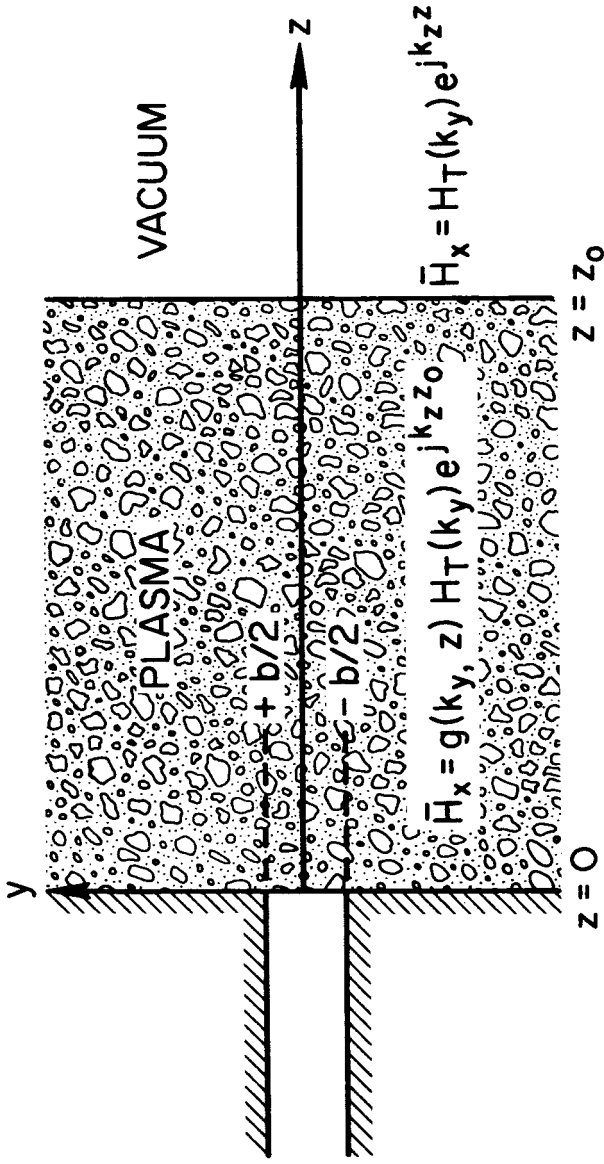
(c) f = 10.8 gc

β	$\dfrac{g(\beta,0)}{g'(\beta,0)}$	$\dfrac{f'(\beta,0)}{f(\beta,0)}$
0	0.070 + j0.200	-0.280 - j0.983
0.100	0.074 + j0.230	-0.290 - j0.973
0.200	0.055 + j0.349	-0.320 - j0.943
0.250	-0.020 + j0.446	-0.342 - j0.921
0.300	-0.188 + j0.498	-0.370 - j0.894
0.350	-0.364 + j0.410	-0.403 - j0.863
0.400	-0.422 + j0.261	-0.442 - j0.827
0.450	-0.402 + j0.153	-0.486 - j0.787
0.500	-0.365 + j0.093	-0.536 - j0.743
0.530	-0.344 + j0.070	-0.469 - j0.715
0.570	-0.320 + j0.050	-0.615 - j0.676
0.600	-0.304 + j0.039	-0.653 - j0.645
0.630	-0.291 + j0.032	-0.693 - j0.612
0.670	-0.275 + j0.024	-0.749 - j0.567
0.700	-0.266 + j0.020	-0.794 - j0.532
0.725	-0.259 + j0.017	-0.833 - j0.502
0.750	-0.252 + j0.015	-0.873 - j0.471
0.775	-0.246 + j0.013	-0.916 - j0.440
0.800	-0.241 + j0.011	-0.959 - j0.407
0.820	-0.237 + j0.010	-0.995 - j0.380
0.840	-0.233 + j0.009	-1.032 - j0.353
0.860	-0.230 + j0.008	-1.070 - j0.324
0.880	-0.226 + j0.008	-1.109 - j0.295
0.900	-0.223 + j0.007	-1.149 - j0.264
0.920	-0.221 + j0.006	-1.190 - j0.232
0.940	-0.218 + j0.006	-1.232 - j0.197
0.960	-0.215 + j0.005	-1.275 - j0.157
0.970	-0.214 + j0.005	-1.297 - j0.135
0.980	-0.213 + j0.005	-1.319 - j0.109
0.990	-0.212 + j0.005	-1.341 - j0.077
0.995	-0.211 + j0.004	-1.352 - j0.055
1.000	-0.210 + j0.004	-1.364 - j0.002
1.200	-0.191 + j0.002	-2.102 - j0.001
1.500	-0.172 + j0.001	-2.893 - j0.001
2.000	-0.148 + j0.001	-4.121 - j0.000
2.500	-0.129 + j0.000	-5.313 - j0.000
3.000	-0.114 + j0.000	-6.488 - j0.000
3.500	-0.102 + j0.000	-7.654 - j0.000
4.000	-0.092 + j0.000	-8.812 - j0.000

TABLE I.- TABLES OF $\dfrac{g(\beta,0)}{g'(\beta,0)}$ AND $\dfrac{f'(\beta,0)}{f(\beta,0)}$ FOR THE INHOMOGENEOUS
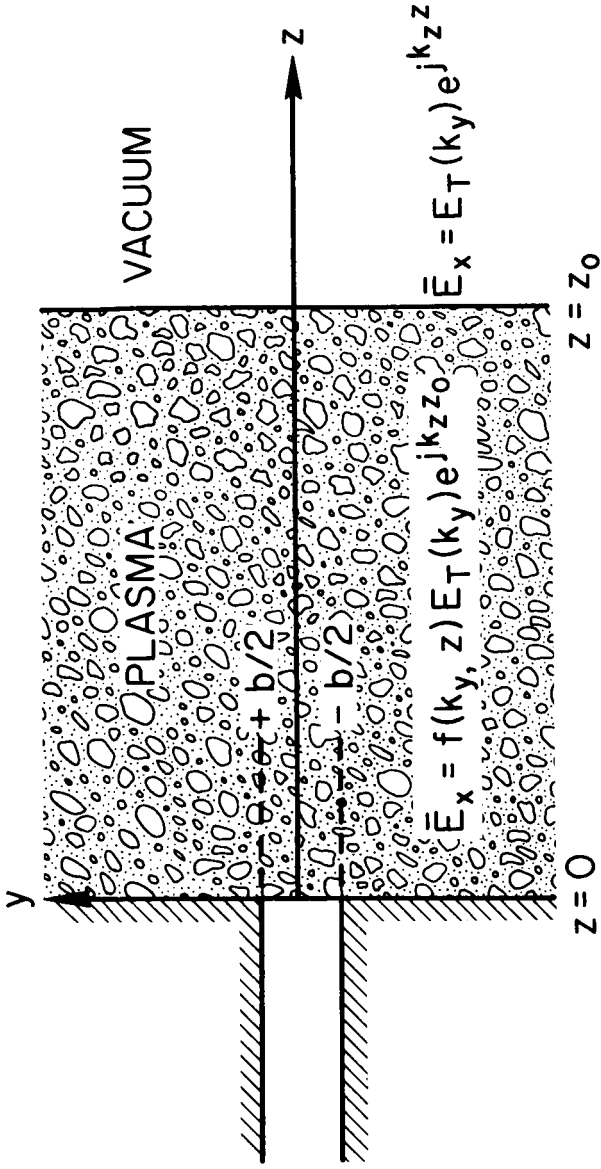
PLASMA GIVEN IN FIGURE 7 - Concluded

(d) f = 11.4 gc

β	$\dfrac{g(\beta,0)}{g'(\beta,0)}$	$\dfrac{f'(\beta,0)}{f(\beta,0)}$
0	0.030 + j0.194	-0.168 - j1.099
0.050	0.031 + j0.196	-0.170 - j1.096
0.100	0.033 + j0.202	-0.178 - j1.087
0.150	0.037 + j0.212	-0.192 - j1.073
0.200	0.041 + j0.228	-0.211 - j1.053
0.225	0.044 + j0.238	-0.222 - j1.041
0.250	0.046 + j0.251	-0.235 - j1.028
0.275	0.048 + j0.265	-0.250 - j1.013
0.300	0.050 + j0.283	-0.266 - j0.997
0.325	0.050 + j0.304	-0.283 - j0.979
0.350	0.049 + j0.329	-0.302 - j0.960
0.375	0.044 + j0.358	-0.322 - j0.940
0.400	0.035 + j0.392	-0.344 - j0.919
0.425	0.019 + j0.431	-0.367 - j0.897
0.450	-0.008 + j0.474	-0.392 - j0.873
0.475	-0.049 + j0.518	-0.418 - j0.849
0.500	-0.108 + j0.558	-0.446 - j0.823
0.550	-0.277 + j0.588	-0.507 - j0.768
0.600	-0.449 + j0.502	-0.575 - j0.710
0.650	-0.529 + j0.346	-0.649 - j0.648
0.700	-0.520 + j0.210	-0.730 - j0.582
0.800	-0.429 + j0.071	-0.914 - j0.441
0.900	-0.353 + j0.024	-1.125 - j0.283
1.000	-0.303 + j0.002	-1.364 - j0.002
1.200	-0.239 + j0.001	-2.160 - j0.001
1.400	-0.208 + j0.001	-2.737 - j0.001
1.600	-0.187 + j0.000	-3.279 - j0.001
1.800	-0.170 + j0.000	-3.805 - j0.000
2.000	-0.157 + j0.000	-4.322 - j0.000
2.500	-0.133 + j0.000	-5.589 - j0.000
3.000	-0.115 + j0.000	-6.836 - j0.000
3.500	-0.101 + j0.000	-8.069 - j0.000
4.000	-0.091 + j0.000	-9.294 - j0.000

VACUUM

PLASMA

z

y

$z = z_0$

$z = 0$

$\bar{H}_x = H_T(k_y) e^{jk_z z}$

$\bar{H}_x = g(k_y, z) H_T(k_y) e^{jk_z z_0}$

$$\frac{d^2 g}{dz^2} - \frac{1}{\epsilon} \frac{d\epsilon}{dz} \frac{dg}{dz} + \left[\omega^2 \mu_0 \epsilon(z) - k_y^2\right] g = 0$$

$$\begin{Bmatrix} \bar{H}_x(k_y, o) \\ E_y(k_y, o) \end{Bmatrix} = \begin{bmatrix} g(k_y, o) \\ \dfrac{-jg'(k_y, o)}{k_0 Y_0 \dfrac{\epsilon(0)}{\epsilon_0}} \end{bmatrix} H_T(k_y) e^{jk_z z_0}$$
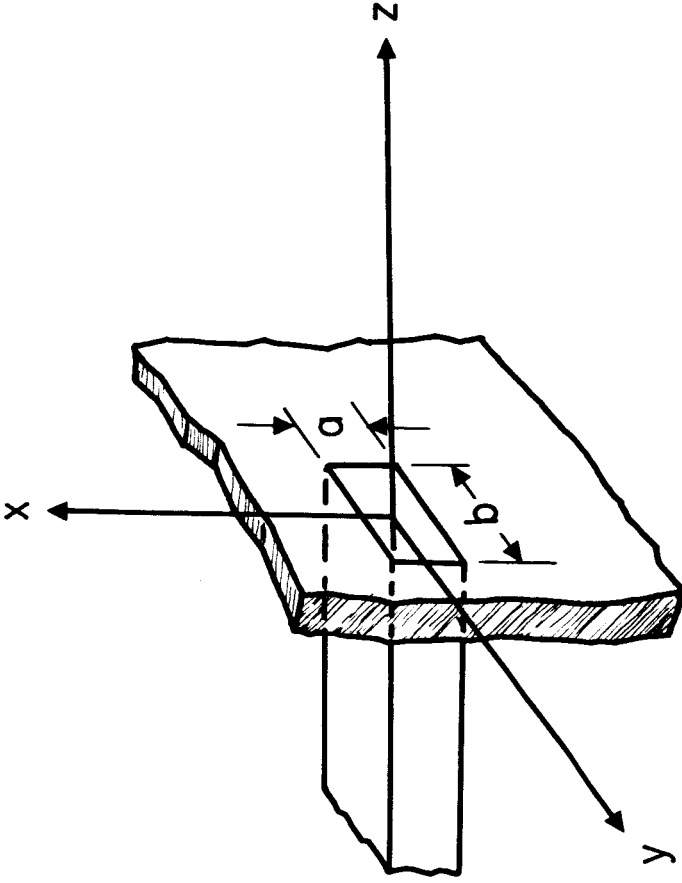
Figure 1.- Plasma covered TE_x slot.

VACUUM

z

$\bar{E}_x = E_T(k_y) e^{jk_z z}$

$z = z_o$

PLASMA

$y = c + b/2$

$y = c - b/2$

$\bar{E}_x = f(k_y, z) E_T(k_y) e^{jk_z z_o}$

y

$z = 0$

$$\frac{d^2 f}{dz^2} + \left[\omega^2 \mu_o \epsilon(z) - k_y{}^2 \right] f = 0$$

$$\left\{ \begin{array}{c} \bar{E}_x(k_y, o) \\ \bar{H}_y(k_y, o) \end{array} \right\} = \left[\begin{array}{c} f(k_y, o) \\ \dfrac{-f'(k_y, o)}{j\omega\mu_o} \end{array} \right] E_T(k_y) e^{jk_z z_o}$$

Figure 2.- Plasma covered TM_x slot.

$$Y = \int_0^\infty \beta \, d\beta \int_0^{2\pi} d\alpha \; F \left[\frac{g(\beta,o)}{g'(\beta,o)} \; , \; \frac{f'(\beta,o)}{f(\beta,o)} \; , \; \alpha \right]$$
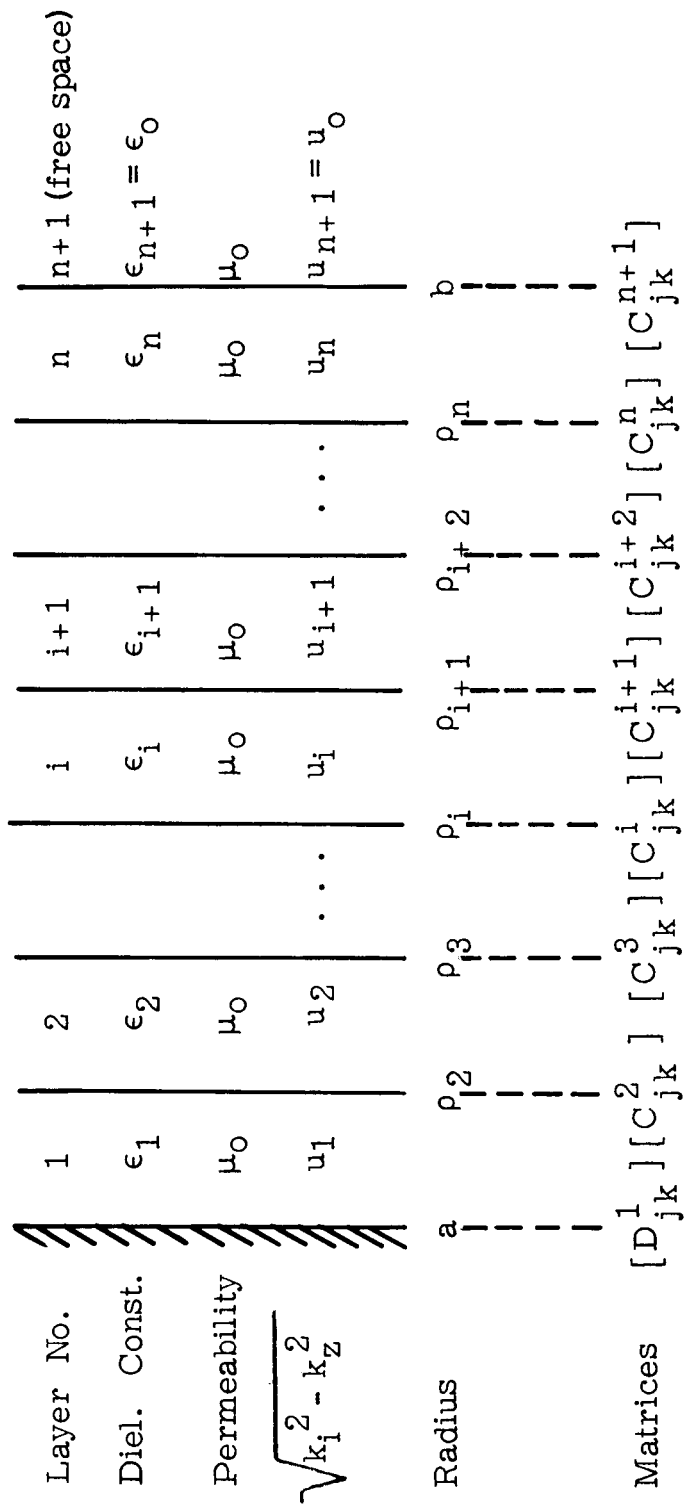
Figure 3.- Aperture coated with inhomogeneous plasma.
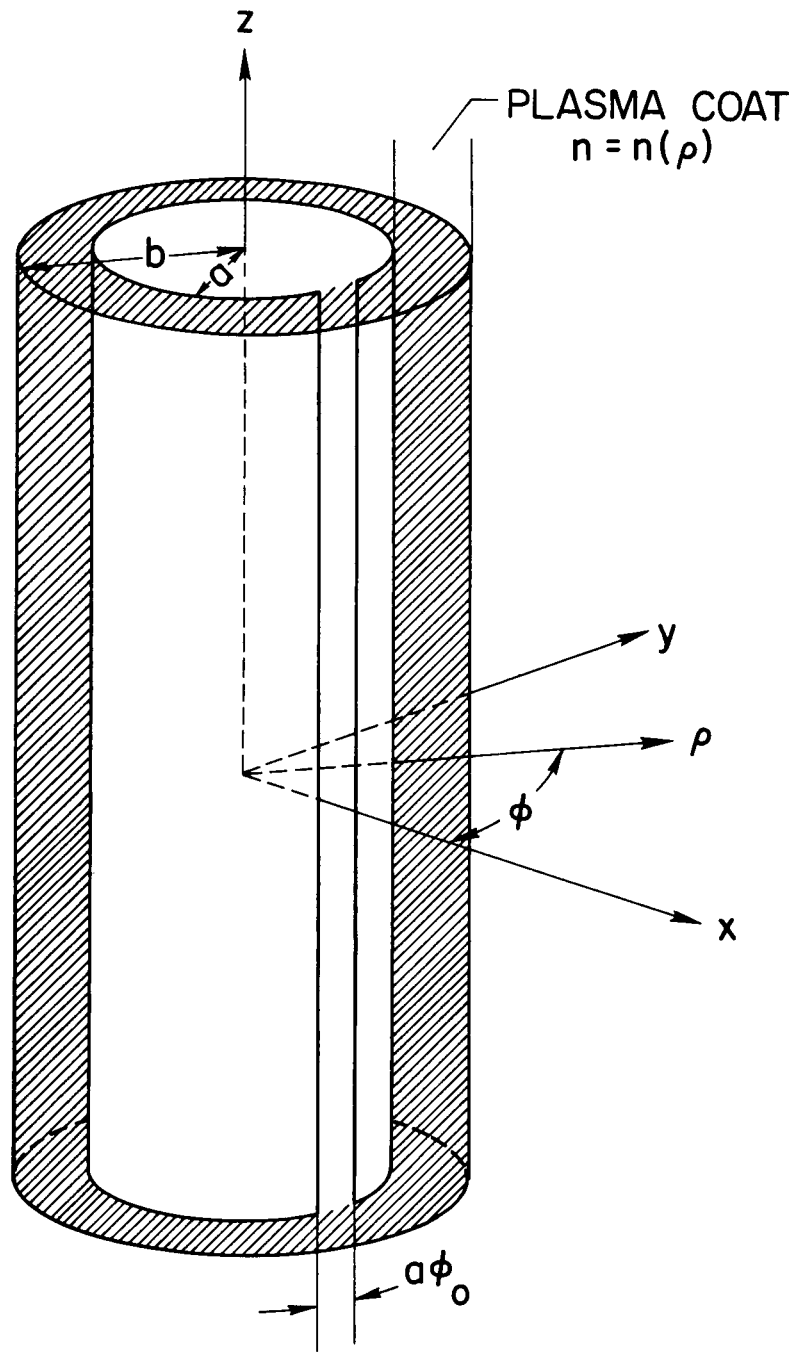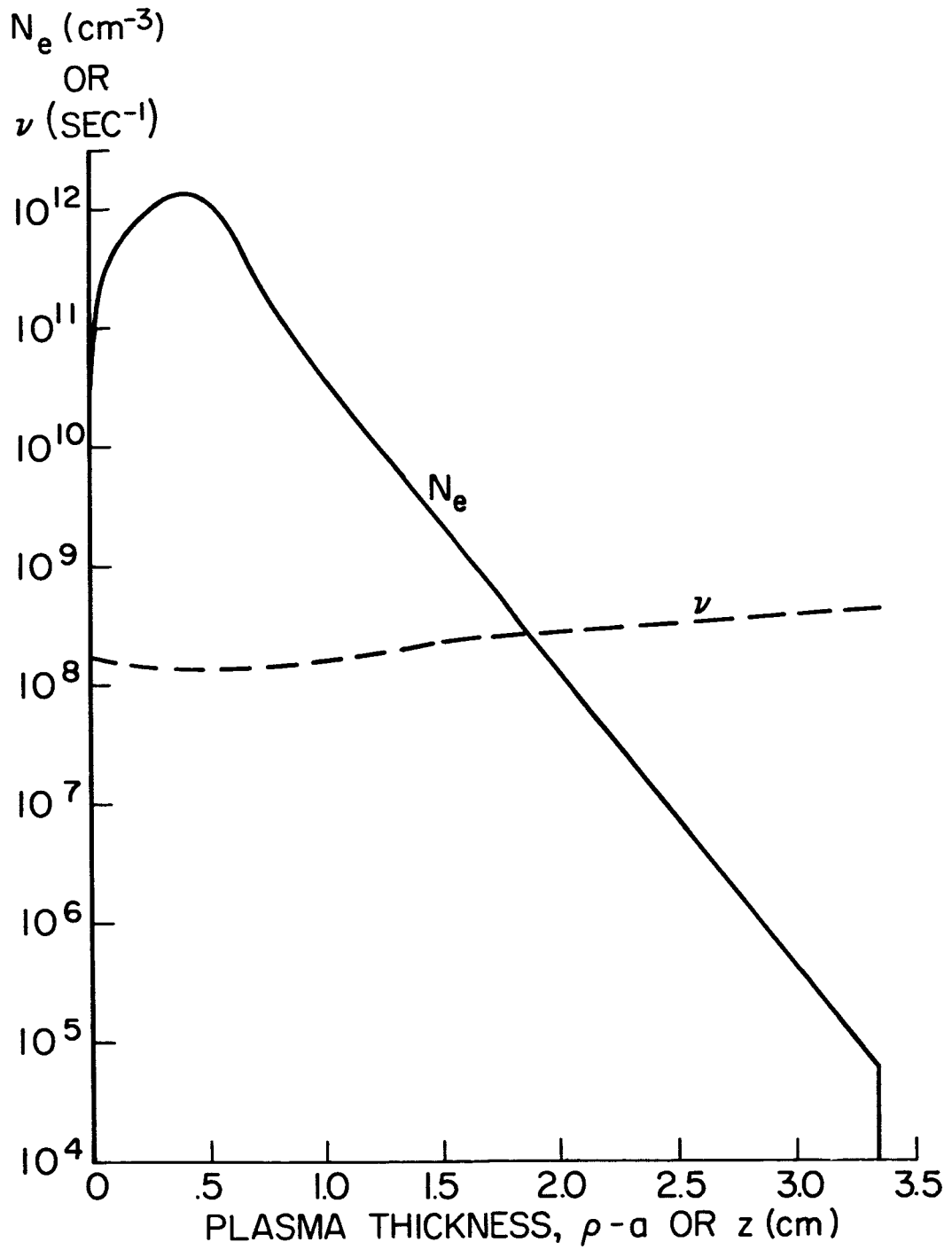
Figure 4.- Geometry of a coated slotted cylinder.
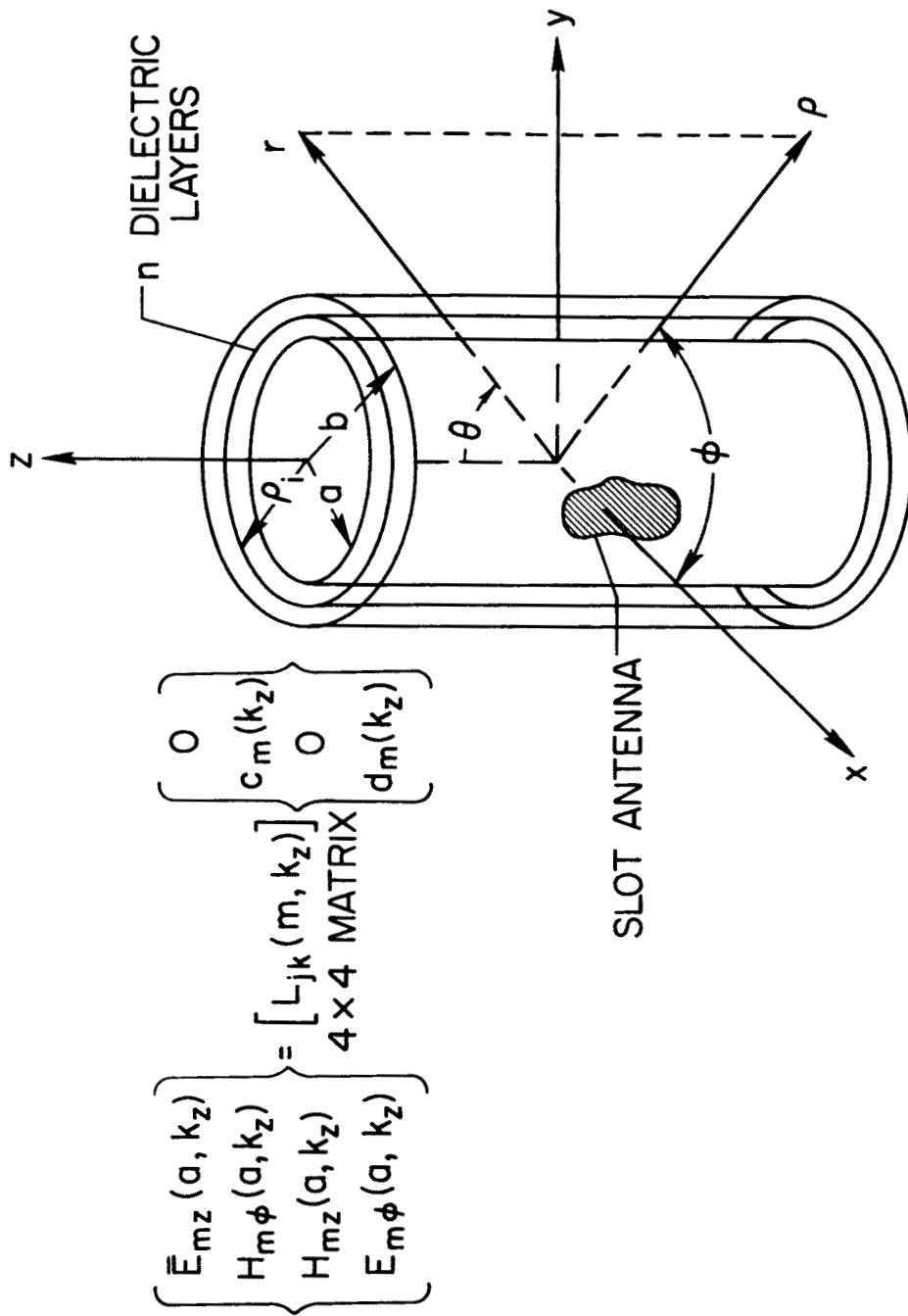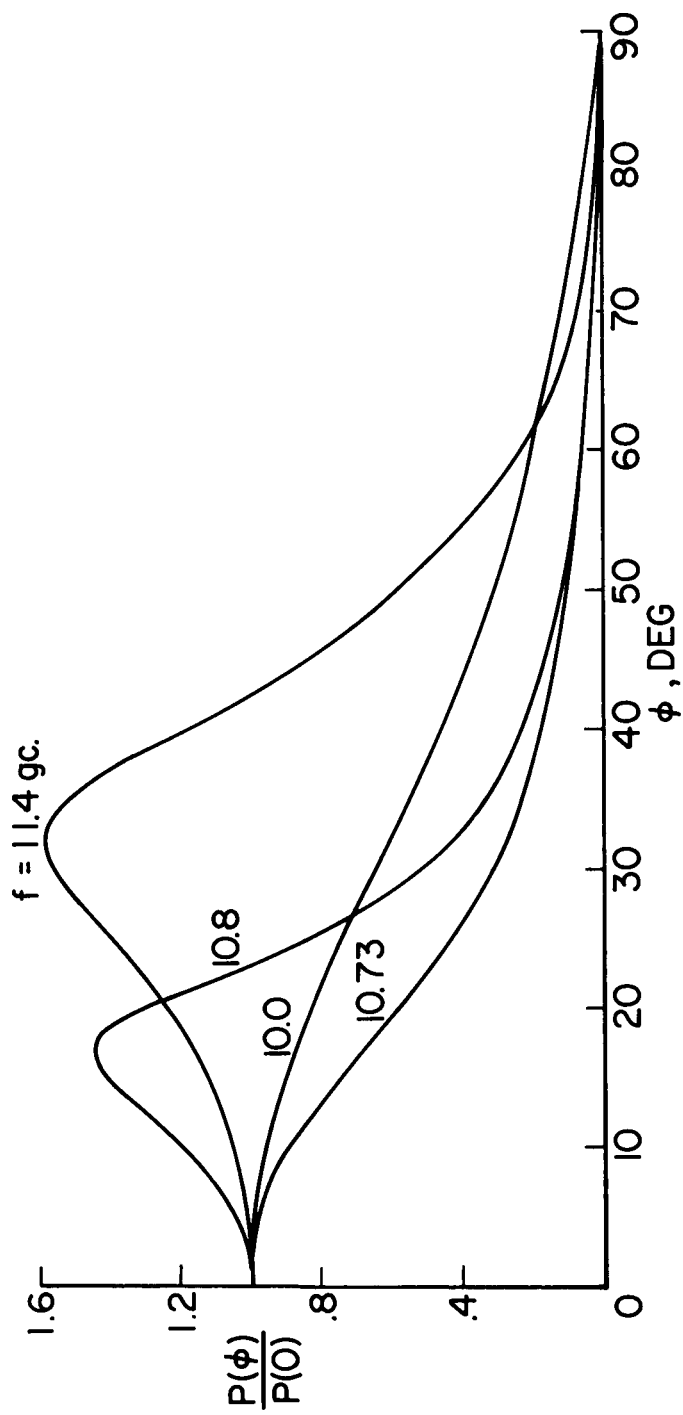
NASA

Figure 5.— General aperture on a coated cylinder.

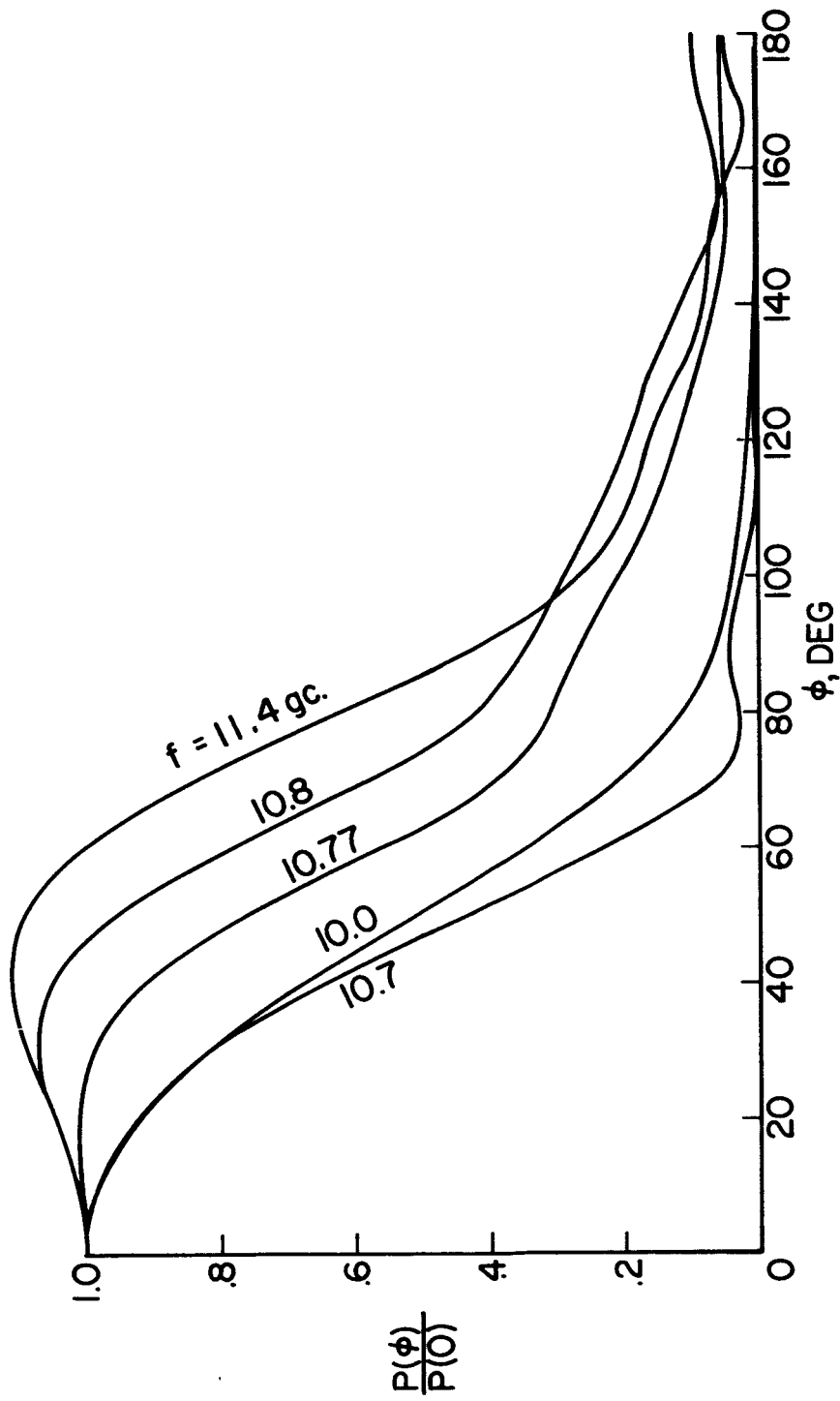| Layer No.	1	2		i	i+1		n	n+1 (free space)
Diel. Const.	ϵ_1	ϵ_2		ϵ_i	ϵ_{i+1}		ϵ_n	$\epsilon_{n+1} = \epsilon_O$
Permeability	μ_O	μ_O		μ_O	μ_O		μ_O	μ_O
$\sqrt{k_i^2 - k_z^2}$	u_1	u_2		u_i	u_{i+1}		u_n	$u_{n+1} = u_O$
Radius	a	ρ_2	ρ_3	ρ_i	ρ_{i+1}	ρ_{i+2}	ρ_n	b
Matrices	$[D_{jk}^1]$	$[C_{jk}^2]$	$[C_{jk}^3]$	$[C_{jk}^i]$	$[C_{jk}^{i+1}]$	$[C_{jk}^{i+2}]$	$[C_{jk}^n]$	$[C_{jk}^{n+1}]$

Figure 6.- Schematic for applying boundary conditions.

NASA

Figure 7.- Typical reentry plasma profile.

NASA

Figure 8.- Patterns of the coated slotted plane.

Figure 9.- Patterns of the coated slotted cylinder.
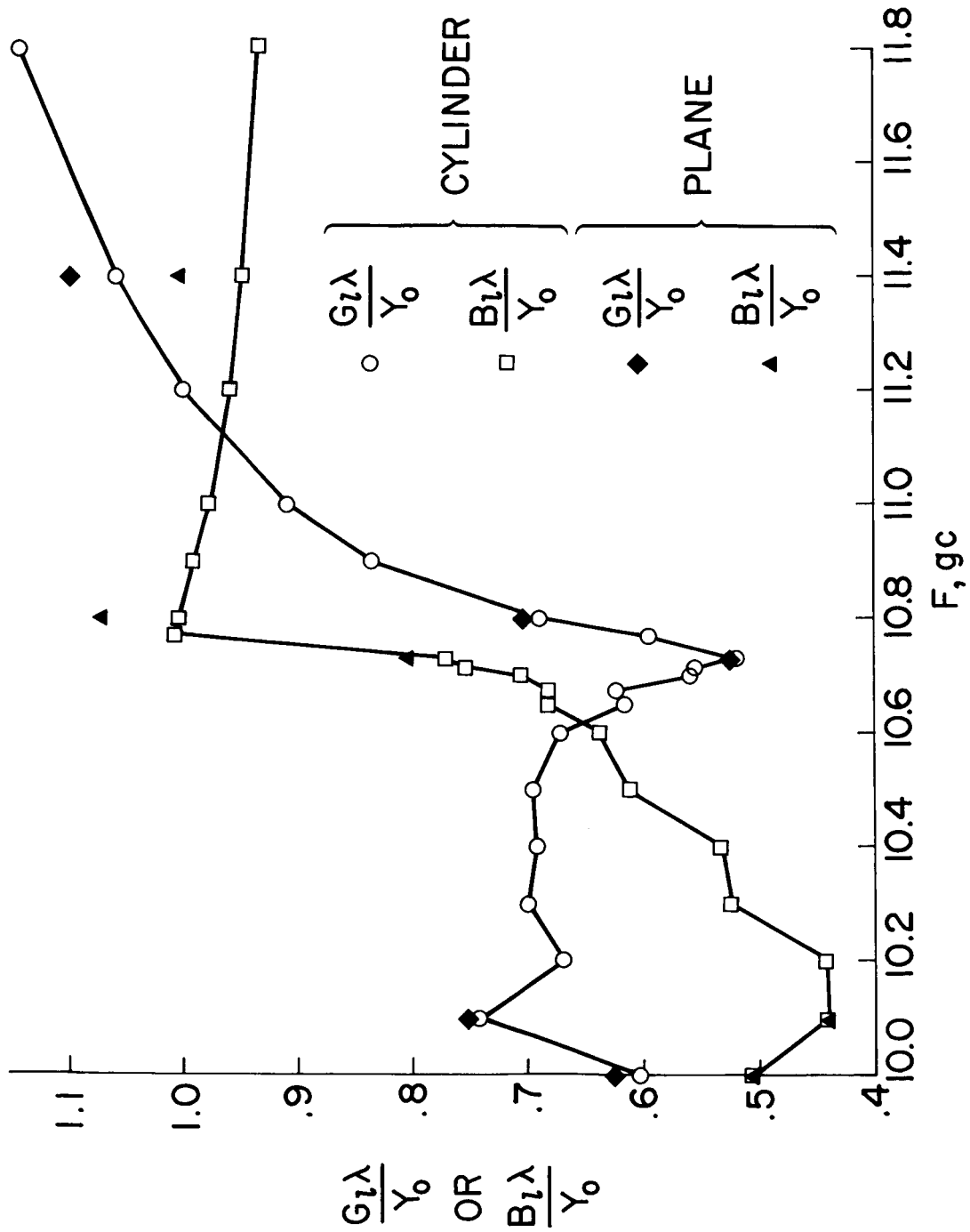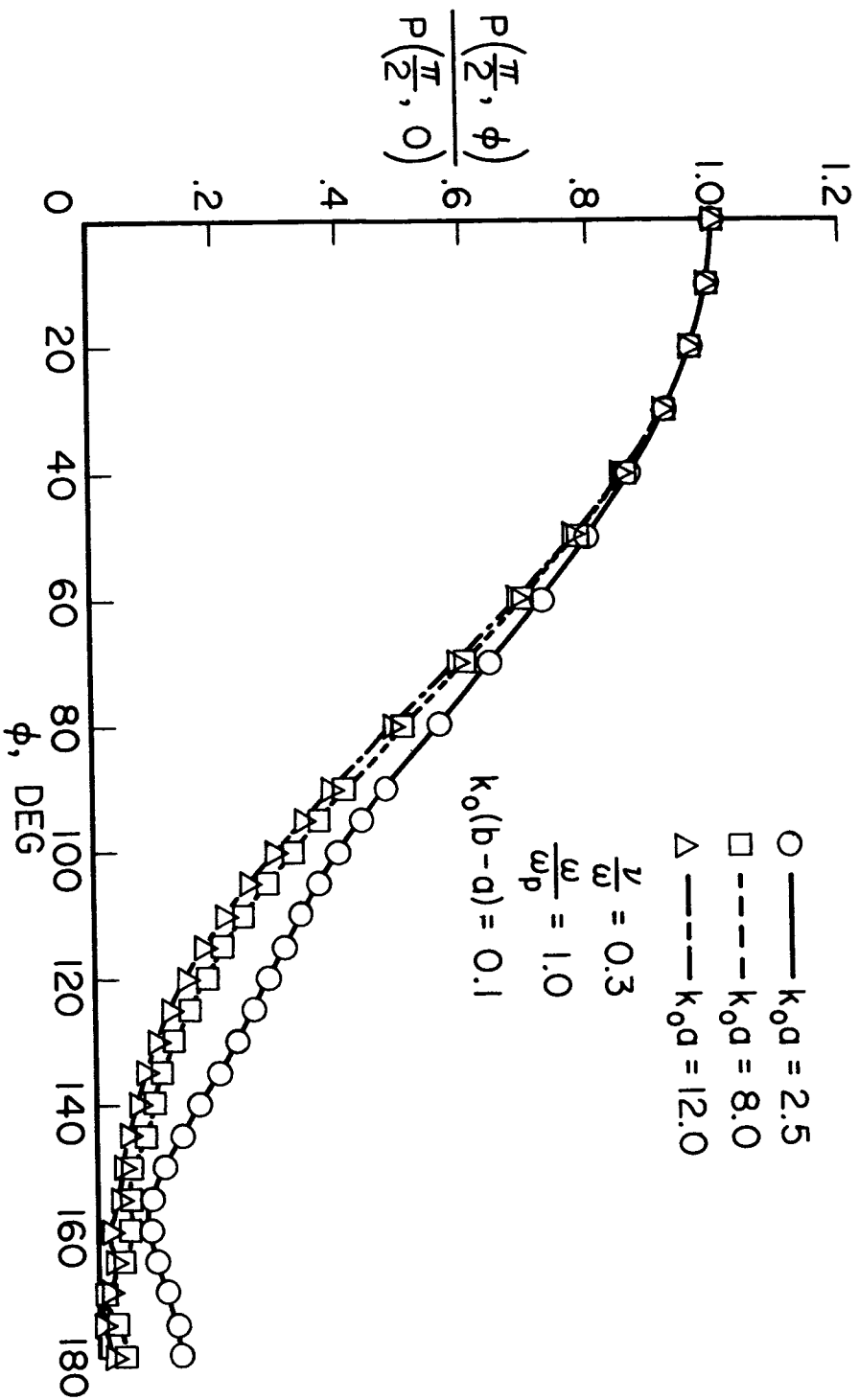
NASA

Figure 10.- Admittance of coated slots.

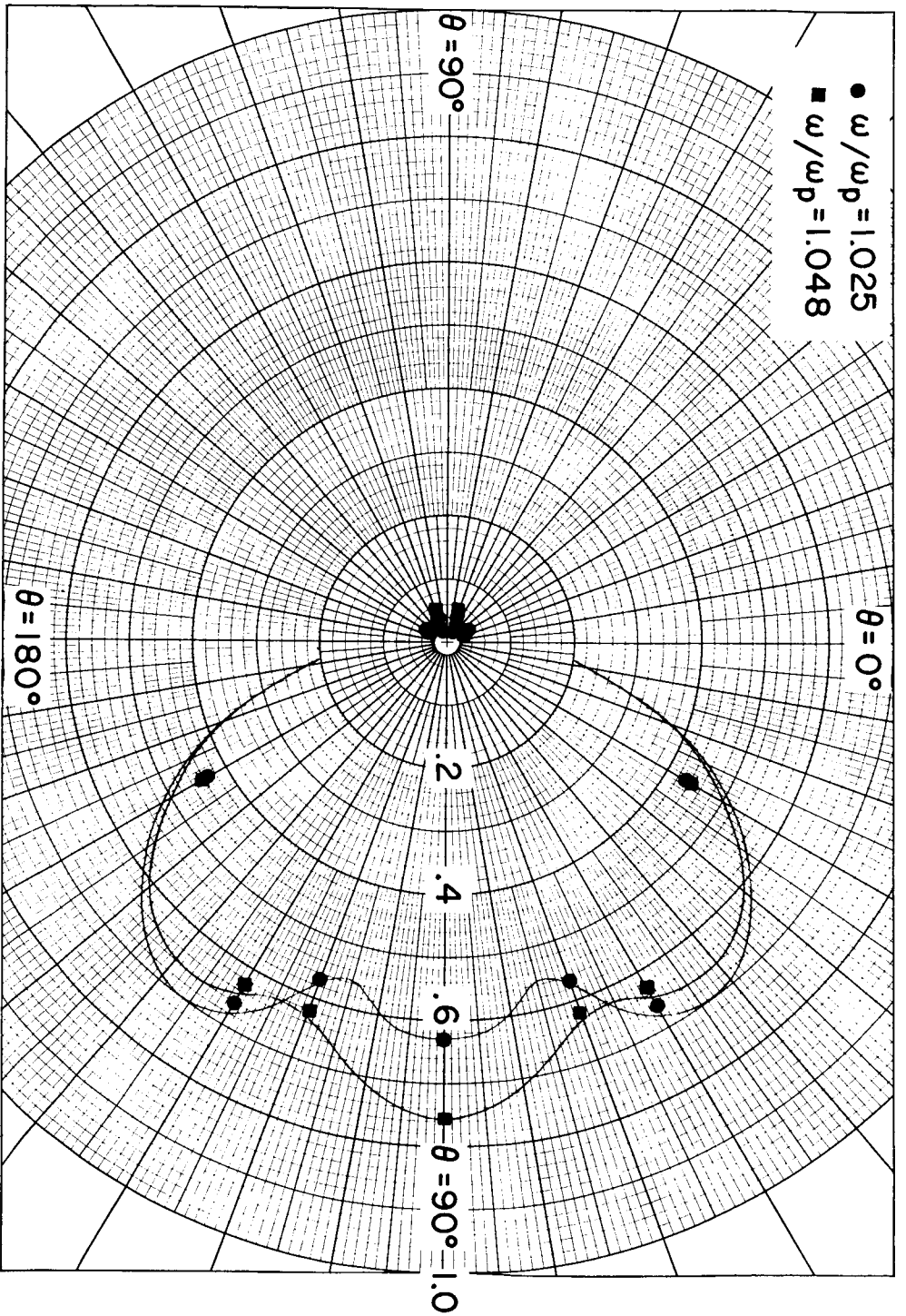Figure 11.— Equatorial patterns of coated axially slotted cylinders.

Figure 12.— Elevation patterns of a coated axially slotted cylinder.

- $\omega / \omega_p = 1.025$
- $\omega / \omega_p = 1.048$

$\theta = 0°$

$\theta = 90°$

$\theta = 180°$

$.2$

$.4$

$.6$

$\theta = 90° = 1.0$